THE BRAIDER

No.43 **AUGUST 2005.**

CONTENTS

A quarterly publication
for
the braiding artisan

Resale of this publication or copies thereof
is strictly prohibited

This publication is available to braiding artisans only.

Copies may be obtained from:

A.G. Schaake,
21 Sundown Cresc.,
Hamilton,
New Zealand.

THE BRAIDER'S NOTEBOOK

In *The Braider*, Issue No. 41, we discussed the Regular Cylindrical Braids with an even number of bights of which a string passes diametrically through its supporting object. In this issue we will look at the Regular Nested Cylindrical Braids with an even number of bights of which a string passes diametrically through its supporting object.

The Standard and Semi-Standard Herringbone Pineapple Knots:

We like to stress that it is essential to draw the grid-diagrams of the knots involved. This will then enable us to determine of which component knot the string-run should pass diametrically through the object to be covered by the Standard Herringbone Pineapple Knot.

Example 1.

Let $A = 2$, $x = 10$, $B^* = 6$. Hence $k = \left|\frac{x+A}{2} - 1\right|_A = \left|\frac{10+2}{2} - 1\right|_2 = |5|_2 = 1$.†

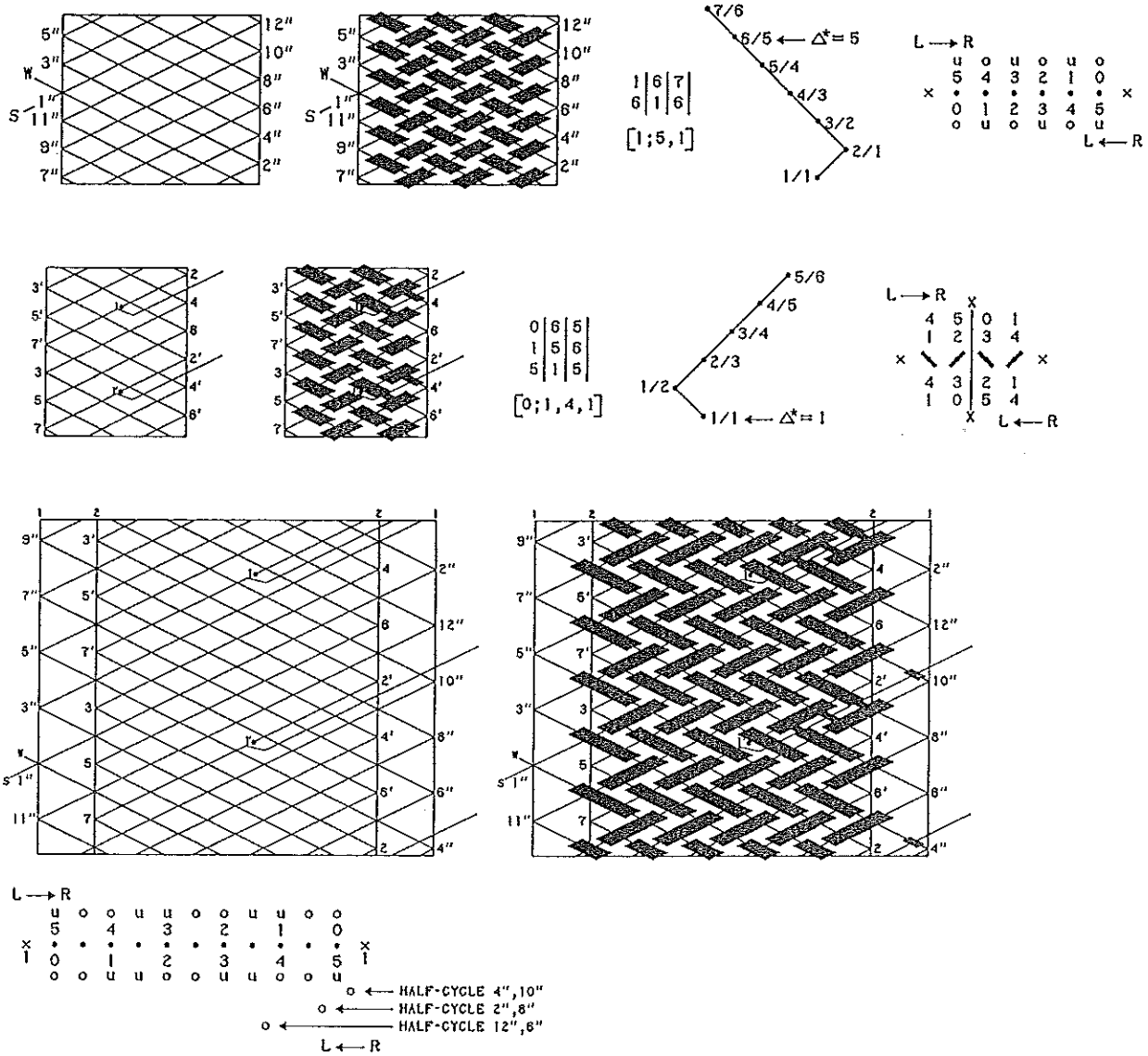

Fig. 781 — Example 1. -- the knots involved.

† See *The Braider*, Issue No. 23, pg. 521.

The coding of the lowermost right-hand grid-diagram shows that the component between left bight-boundary 2 and right bight-boundary 2 is the preferred one for having its string diametrically through the object over which the 2-pass Standard Herringbone Pineapple Knot is meant to sit. This component (an over-under coded Regular Knot) has 5-parts and 6-bights. Say we braid this component in the parallel braiding way. Then its half-cycle braiding algorithms are as follows:

half-cycle parts 1 & 1′ :		:	$L \longrightarrow R$:	Free run.
half-cycles 2 & 2′ :	$i = 0$;	$i \neq 0$ left of X–X :	$L \longleftarrow R$:	Free run.
half-cycles 3 & 3′ :	$i = 0$;	:	$L \longrightarrow R$:	u.
half-cycles 4 & 4′ :	$i \leq 1$;	$i \neq 1$ left of X–X :	$L \longleftarrow R$:	$2u$.
half-cycles 5 & 5′ :	$i \leq 1$;	:	$L \longrightarrow R$:	$2u - o$.
half-cycles 6 & 6′ :	$i \leq 2$;	$i \neq 2$ left of X–X :	$L \longleftarrow R$:	$u - o - u - o$.
half-cycles 7 & 7′ :	$i \leq 2$;	:	$L \longrightarrow R$:	$u - o - 2u$.

Next we interbraid the component between left bight-boundary 1 and right bight-boundary 1. This component (an over-under coded Regular Knot) has 7-parts and 6-bights. Its algorithm diagram as the interbraid is shown below the lowermost string-run diagram and grid-diagram from which we read its half-cycle braiding algorithms:

half-cycle 1″ :	;	$L \longrightarrow R$:	$o - u - o - u - o$.
half-cycle 2″ :	$i = 0$;	$L \longleftarrow R$:	$2o - u - o - u - 2o$.
half-cycle 3″ :	$i = 0$;	$L \longrightarrow R$:	$o - u - o - u - 2o$.
half-cycle 4″ :	$i \leq 1$;	$L \longleftarrow R$:	$2o - u - o - 2u - 2o$.
half-cycle 5″ :	$i \leq 1$;	$L \longrightarrow R$:	$o - u - o - 2u - 2o$.
half-cycle 6″ :	$i \leq 2$;	$L \longleftarrow R$:	$2o - u - 2o - 2u - 2o$.
half-cycle 7″ :	$i \leq 2$;	$L \longrightarrow R$:	$o - u - 2o - 2u - 2o$.
half-cycle 8″ :	$i \leq 3$;	$L \longleftarrow R$:	$2o - 2u - 2o - 2u - 2o$.
half-cycle 9″ :	$i \leq 3$;	$L \longrightarrow R$:	$o - 2u - 2o - 2u - 2o$.
half-cycle 10″ :	$i \leq 4$;	$L \longleftarrow R$:	$3o - 2u - 2o - 2u - 2o$.
half-cycle 11″ :	$i \leq 4$;	$L \longrightarrow R$:	$2o - 2u - 2o - 2u - 2o$.
half-cycle 12″ :	$i \leq 5$;	$L \longleftarrow R$:	$u - 3o - 2u - 2o - 2u - 2o$.

Although the above procedure, using the lowermost algorithm diagram form in Fig. 781 for obtaining the half-cycle braiding algorithms for interbraiding the second component, is suitable for 2-pass Standard Herringbone Pineapple Knots, it is in general not suitable for Standard or Semi-Standard Herringbone Pineapple Knots for which $A > 2$. After obtaining the half-cycle braiding algorithms for the foundation knot (the knot of which the string passes diametrically through the object over which it sits) we obtain the half-cycle braiding algorithms for the further interbraided components by the appropriate modifications of their half-cycle braiding algorithms associated with a normal braided foundation knot. In our Example above, the half-cycle braiding algorithms for the interbraided component between left bight-boundary 1 and right bight-boundary 1, associated with a normal braided foundation knot, are obtained from the following algorithm diagram[†]:

$\longrightarrow$	$l_i - 1$	$A - 1$	$A - 1$	$A - 1$	$A - 1$	$A - 1$	$r_i - 1$
0	$\star$	$\star$	$\star$	$\star$	$\star$	$\star$	
/	\	/	\	/	\	/	\
	$\star$	$\star$	$\star$	$\star$	$\star$	$\star$	0
$l_i - 1$	$A - 1$	$A - 1$	$A - 1$	$A - 1$	$A - 1$	$r_i - 1$	$\longleftarrow$

[†] See *The Braider*, Issue No. 27, pg. 634.

where the positions of the stars are being occupied by the i-values of the complementary bight-number scheme associated with the component to be interbraided, and where the reference value above an upper star, or below a lower star, increases by 1 when its associated i-value is applicable to the half-cycle concerned, excepting the **last** entry $(r_i - 1)u$ which remains the same for each of the lower-left to upper-right half-cycles, and the **last** entry $(l_i - 1)u$ which remains the same for each of the lower-right to upper-left half-cycles. Hence, since $r_i = 1$, $l_i = 1$ and $\Delta^* = 5$ for $p/b = 7/6$, from the algorithm diagram:

$\longrightarrow$	0	1	1	1	1	1	0
$\vdash$	5	4	3	2	1	0	
/	\	/	\	/	\	/	\
	0	1	2	3	4	5	$\dashv$
0	1	1	1	1	1	0	$\longleftarrow$

This algorithm diagram gives us the following half-cycle braiding algorithms:

half-cycle $1''$:	;	$L \longrightarrow R$:	$o - u - o - u - o$.
half-cycle $2''$:	$i = 0$;	$L \longleftarrow R$:	$o - u - o - u - 2o$.
half-cycle $3''$:	$i = 0$;	$L \longrightarrow R$:	$o - u - o - u - 2o$.
half-cycle $4''$:	$i \leq 1$;	$L \longleftarrow R$:	$o - u - o - 2u - 2o$.
half-cycle $5''$:	$i \leq 1$;	$L \longrightarrow R$:	$o - u - o - 2u - 2o$.
half-cycle $6''$:	$i \leq 2$;	$L \longleftarrow R$:	$o - u - 2o - 2u - 2o$.
half-cycle $7''$:	$i \leq 2$;	$L \longrightarrow R$:	$o - u - 2o - 2u - 2o$.
half-cycle $8''$:	$i \leq 3$;	$L \longleftarrow R$:	$o - 2u - 2o - 2u - 2o$.
half-cycle $9''$:	$i \leq 3$;	$L \longrightarrow R$:	$o - 2u - 2o - 2u - 2o$.
half-cycle $10''$:	$i \leq 4$;	$L \longleftarrow R$:	$2o - 2u - 2o - 2u - 2o$.
half-cycle $11''$:	$i \leq 4$;	$L \longrightarrow R$:	$2o - 2u - 2o - 2u - 2o$.
half-cycle $12''$:	$i \leq 5$;	$L \longleftarrow R$:	$u - 2o - 2u - 2o - 2u - 2o$.

From the grid-diagram in Fig. 781 we see that for these half-cycles:
half-cycle $2''$ has one additional o before the first o.
half-cycle $4''$ has one additional o before the first o.
half-cycle $6''$ has one additional o after the first o.
half-cycle $8''$ has one additional o before the first o.
half-cycle $10''$ has one additional o before the first $2o$.
half-cycle $12''$ has one additional o after the first $2o$.

After making these adjustments we obtain the half-cycle braiding algorithms on pg. 1006.

Instead of using the algorithm diagrams in Fig. 781, it is simpler to make use of algorithm diagrams which show all the columns between left bight-boundary 1 and right bight-boundary 1. The bigger dots in such an algorithm diagram indicate the actual intersection columns associated with the component under consideration. The uppermost algorithm diagram in Fig. 782 is associated with the first component, the foundation knot, between left bight-boundary 2 and right bight-boundary 2. The lowermost algorithm diagram in Fig. 782 is associated with the second component between left bight-boundary 1 and right bight-boundary 1. The intersection between a lower-right to upper-left half-cycle of the second component with the outgoing half-cycle parts 7 & $7'$ of the foundation knot (which are **over**-crossings) are indicated by the i-value of the lower-right to upper-left half-cycle concerned (very small + sign with its associated small numeral for the i-value concerned indicates the position of this intersection (readily obtainable from the lowermost string-run diagram in Fig. 781)).

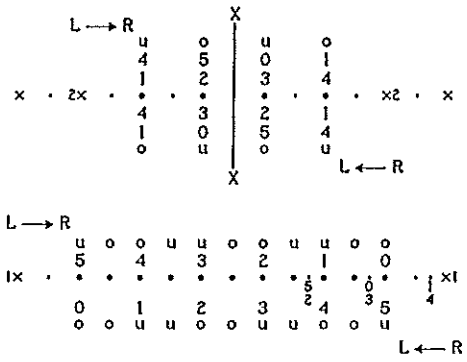

Fig. 782 — The algorithm diagrams showing all the columns between bight-boundaries $l_i = 1$ and $r_i = 1$.

Example 2.

Let $A = 5$, $x = 13$, $B^* = 6$. Hence $k = \left|\frac{x+A}{2} - 1\right|_A = \left|\frac{13+5}{2} - 1\right|_5 = |8|_5 = 3$. We have three components with n-parts and two components with $(n-2)$-parts, and since the total number of parts is $2A + x - 2 = 21$, it follows that $5n = 25$, hence $n = 5$. Thus we have three components with 5-parts and two components with 3-parts. Since g.c.d. $(3, B^*) =$ g.c.d. $(3, 6) = 3$, each of the two components with 3-parts require three essential strings, hence each consists of 3 sub-components with each sub-component having 1-part. We are thus dealing with a Semi-Standard Herringbone Pineapple Knot.

In fact we have met this Semi-Standard Herringbone Pineapple Knot in *The Braider*, Issue No. 27, pp. 629-633, where it was braided in the normal way. There the foundation knot was the component between left bight-boundary 1 and right bight-boundary 3, the second component between left bight-boundary 2 and right bight-boundary 2, the third component between left bight-boundary 3 and right bight-boundary 1, the sub-components of the fourth component between left bight-boundary 5 and right bight-boundary 4, and the sub-components of the fifth component between left bight-boundary 4 and right bight-boundary 5.

Let's now braid this Semi-Standard Herringbone Pineapple Knot with the foundation knot between left bight-boundary 2 and right bight-boundary 2, the string-run of which passes diametrically through the object over which this Semi-Standard Herringbone Pineapple Knot sits. Then the second component we braid between left bight-boundary 1 and right bight-boundary 3, the third component between bight-boundary 3 and right bight-boundary 1, the sub-components of the fourth component between left bight-boundary 5 and right bight-boundary 4, and the sub-components of the fifth component between left bight-boundary 4 and right bight-boundary 5. See Fig. 783.

Hence the half-cycle braiding algorithms for the foundation knot (the first component) are those of the foundation knot in Example 1 with the replacement of o by u and vice versa except for half-cycles 7 & 7′ where right of line X–X we have unders:

half-cycle parts 1 & 1′ :		:	$L \longrightarrow R$:	Free run.
half-cycles 2 & 2′ :	$i = 0$;	$i \neq 0$ left of X–X :	$L \longleftarrow R$:	Free run.
half-cycles 3 & 3′ :	$i = 0$;	:	$L \longrightarrow R$:	o.
half-cycles 4 & 4′ :	$i \leq 1$;	$i \neq 1$ left of X–X :	$L \longleftarrow R$:	$2o$.
half-cycles 5 & 5′ :	$i \leq 1$;	:	$L \longrightarrow R$:	$2o - u$.
half-cycles 6 & 6′ :	$i \leq 2$;	$i \neq 2$ left of X–X :	$L \longleftarrow R$:	$o - u - o - u$.
half-cycles 7 & 7′ :	$i \leq 2$;	:	$L \longrightarrow R$:	$o - 3u$.

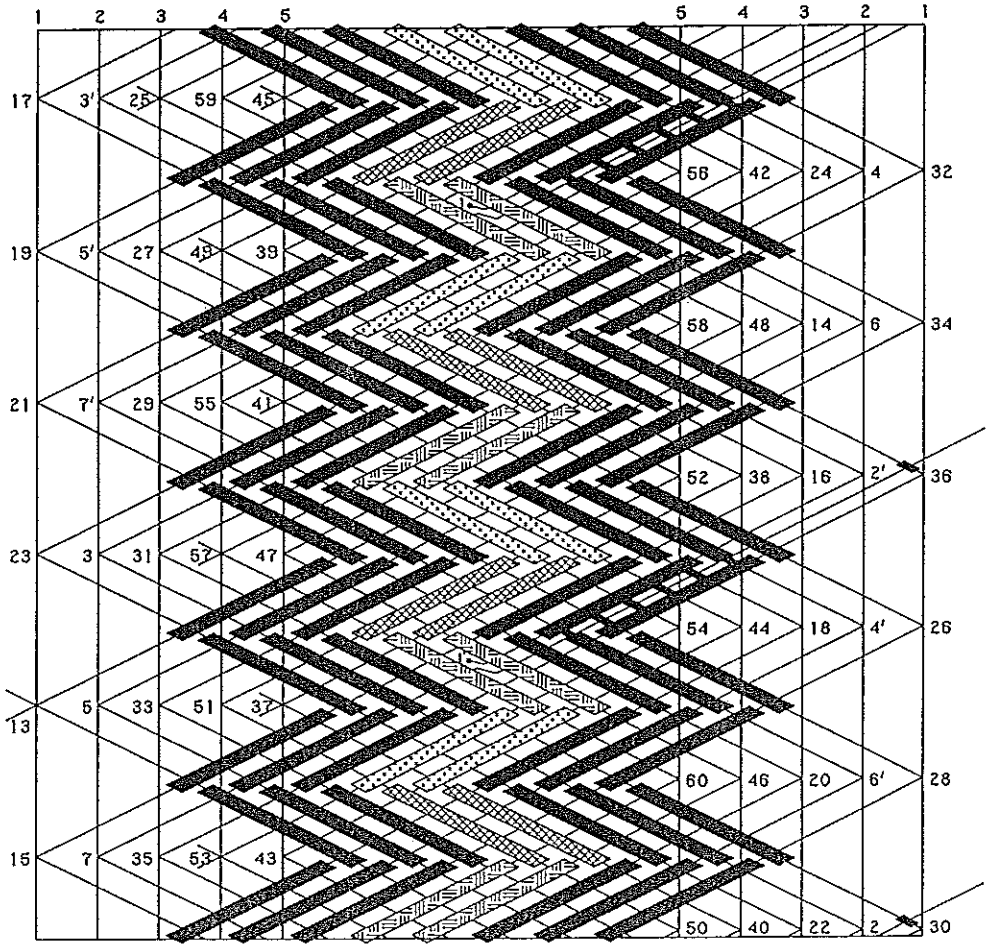

Fig. 783 — The Semi-Standard Herringbone Pineapple Knot of Example 2.

The second component between left bight-boundary 1 and right bight-boundary 3 would have the following half-cycle braiding algorithms when the foundation knot between left bight-boundary 2 and right bight-boundary 2 would have been braided in the normal way without its string going diametrically through the object over which it sits (hence for the second component $A = 2$, $l_i = 1$, $r_i = 2$):

half-cycle 13		:	$L \longrightarrow R$	$o - u - o - u$.
half-cycle 14	$i = 0$	:	$L \longleftarrow R$	$u - o - u - o$.
half-cycle 15	$i = 0$	:	$L \longrightarrow R$	$o - u - o - u$.
half-cycle 16	$i \leq 1$	:	$L \longleftarrow R$	$u - 2o - u - o$.
half-cycle 17	$i \leq 1$	:	$L \longrightarrow R$	$2o - u - o - u$.
half-cycle 18	$i \leq 2$	:	$L \longleftarrow R$	$u - 2o - 2u - o$.
half-cycle 19	$i \leq 2$	:	$L \longrightarrow R$	$2o - 2u - o - u$.
half-cycle 20	$i \leq 3$	:	$L \longleftarrow R$	$u - 2o - 2u - 2o$.
half-cycle 21	$i \leq 3$	:	$L \longrightarrow R$	$2o - 2u - 2o - u$.
half-cycle 22	$i \leq 4$	:	$L \longleftarrow R$	$u - 2o - 2u - 2o - u$.
half-cycle 23	$i \leq 4$	:	$L \longrightarrow R$	$2o - 2u - 2o - 2u$.
half-cycle 24	$i \leq 5$	:	$L \longleftarrow R$	$u - 2o - 2u - 2o - u$.

These half-cycle braiding algorithms and the half-cycle braiding algorithms for the half-cycles 25 to 60 on pp. 632-633 (see *The Braider*, Issue No. 27) have now to be modified as follows:

half-cycle 14 has one additional o before the first o.
half-cycle 18 has one additional o before the first u.
half-cycle 20 has one additional o after the first o.
half-cycle 24 has one additional o before the first u.
half-cycle 26 has one additional o before the first o.
half-cycle 28 has one additional o before the first u.
half-cycle 30 has one additional o before the first o.
half-cycle 32 has one additional o after the first o.
half-cycle 34 has one additional o after the first u.
half-cycle 36 has one additional o before the first o.
half-cycle 42 has one additional o after the first u.
half-cycle 44 has one additional o after the first u.
half-cycle 46 has one additional o after the second o.
half-cycle 48 has one additional o after the second o.
half-cycle 54 has one additional o after the first u.
half-cycle 56 has one additional o after the first u.

Hence the actual half-cycle braiding algorithms for the half-cycles 13 to 60 are as follows:

half-cycle 13		:	$L \longrightarrow R$	$o-u-o-u$.
half-cycle 14	$i=0$	:	$L \longleftarrow R$	$u-2o-u-o$.
half-cycle 15	$i=0$	:	$L \longrightarrow R$	$o-u-o-u$.
half-cycle 16	$i\leq 1$	:	$L \longleftarrow R$	$u-2o-u-o$.
half-cycle 17	$i\leq 1$	:	$L \longrightarrow R$	$2o-u-o-u$.
half-cycle 18	$i\leq 2$	:	$L \longleftarrow R$	$o-u-2o-2u-o$.
half-cycle 19	$i\leq 2$	:	$L \longrightarrow R$	$2o-2u-o-u$.
half-cycle 20	$i\leq 3$	:	$L \longleftarrow R$	$u-3o-2u-2o$.
half-cycle 21	$i\leq 3$	:	$L \longrightarrow R$	$2o-2u-2o-u$.
half-cycle 22	$i\leq 4$	:	$L \longleftarrow R$	$u-2o-2u-2o-u$.
half-cycle 23	$i\leq 4$	:	$L \longrightarrow R$	$2o-2u-2o-2u$.
half-cycle 24	$i\leq 5$	:	$L \longleftarrow R$	$o-u-2o-2u-2o-u$.
half-cycle 25		:	$L \longrightarrow R$	$2u-2o-2u-2o$.
half-cycle 26	$i=0$	:	$L \longleftarrow R$	$3o-2u-2o-2u$.
half-cycle 27	$i=0$	:	$L \longrightarrow R$	$2u-2o-2u-2o$.
half-cycle 28	$i\leq 1$	:	$L \longleftarrow R$	$4o-2u-2o-2u$.
half-cycle 29	$i\leq 1$	:	$L \longrightarrow R$	$2u-3o-2u-2o$.
half-cycle 30	$i\leq 2$	:	$L \longleftarrow R$	$4o-3u-2o-2u$.
half-cycle 31	$i\leq 2$	:	$L \longrightarrow R$	$2u-3o-3u-2o$.
half-cycle 32	$i\leq 3$	:	$L \longleftarrow R$	$4o-3u-3o-2u$.
half-cycle 33	$i\leq 3$	:	$L \longrightarrow R$	$2u-3o-3u-3o$.
half-cycle 34	$i\leq 4$	:	$L \longleftarrow R$	$3o-u-o-2u-3o-3u$.
half-cycle 35	$i\leq 4$	:	$L \longrightarrow R$	$2u-3o-3u-3o-u$.
half-cycle 36	$i\leq 5$	:	$L \longleftarrow R$	$4o-3u-3o-3u$.
half-cycle 37		:	$L \longrightarrow R$	$3u-3o-3u$.
half-cycle 38	$i=0$	:	$L \longleftarrow R$	$3u-3o-3u$.
half-cycle 39	$i=0$	:	$L \longrightarrow R$	$3u-3o-3u$.
half-cycle 40	$i\leq 1$	:	$L \longleftarrow R$	$3u-3o-3u$.
half-cycle 41	$i=X$	:	$L \longrightarrow R$	$3u-4o-3u$.

half-cycle 42	$i = 0\,;\, i = X$	:	$L \longleftarrow R$	$u - o - 2u - 4o - 3u\,.$
half-cycle 43	$i = 0\,;\, i = X$	:	$L \longrightarrow R$	$3u - 4o - 3u\,.$
half-cycle 44	$i \leq 1\,;\, i = X$	:	$L \longleftarrow R$	$u - o - 2u - 4o - 3u\,.$
half-cycle 45	$i = X, Y$	:	$L \longrightarrow R$	$3u - 4o - 4u\,.$
half-cycle 46	$i = 0\,;\, i = X, Y$	:	$L \longleftarrow R$	$3u - 5o - 4u\,.$
half-cycle 47	$i = 0\,;\, i = X, Y$	:	$L \longrightarrow R$	$3u - 4o - 4u\,.$
half-cycle 48	$i \leq 1\,;\, i = X, Y$	:	$L \longleftarrow R$	$3u - 5o - 4u\,.$
half-cycle 49		:	$L \longrightarrow R$	$3u - 4o - 4u\,.$
half-cycle 50	$i = 0$	:	$L \longleftarrow R$	$4u - 4o - 3u\,.$
half-cycle 51	$i = 0$	:	$L \longrightarrow R$	$3u - 4o - 4u\,.$
half-cycle 52	$i \leq 1$	:	$L \longleftarrow R$	$4u - 4o - 3u\,.$
half-cycle 53	$i = X$	:	$L \longrightarrow R$	$3u - 5o - 4u\,.$
half-cycle 54	$i = 0\,;\, i = X$	:	$L \longleftarrow R$	$u - o - 3u - 5o - 3u\,.$
half-cycle 55	$i = 0\,;\, i = X$	:	$L \longrightarrow R$	$3u - 5o - 4u\,.$
half-cycle 56	$i \leq 1\,;\, i = X$	:	$L \longleftarrow R$	$u - o - 3u - 5o - 3u\,.$
half-cycle 57	$i = X, Y$	:	$L \longrightarrow R$	$3u - 5o - 5u\,.$
half-cycle 58	$i = 0\,;\, i = X, Y$	:	$L \longleftarrow R$	$4u - 5o - 4u\,.$
half-cycle 59	$i = 0\,;\, i = X, Y$	:	$L \longrightarrow R$	$3u - 5o - 5u\,.$
half-cycle 60	$i \leq 1\,;\, i = X, Y$	:	$L \longleftarrow R$	$4u - 5o - 4u\,.$

Instead of using the above procedure, it is simpler to make use of algorithm diagrams which show all the columns between left bight-boundary 1 and right bight-boundary 1.

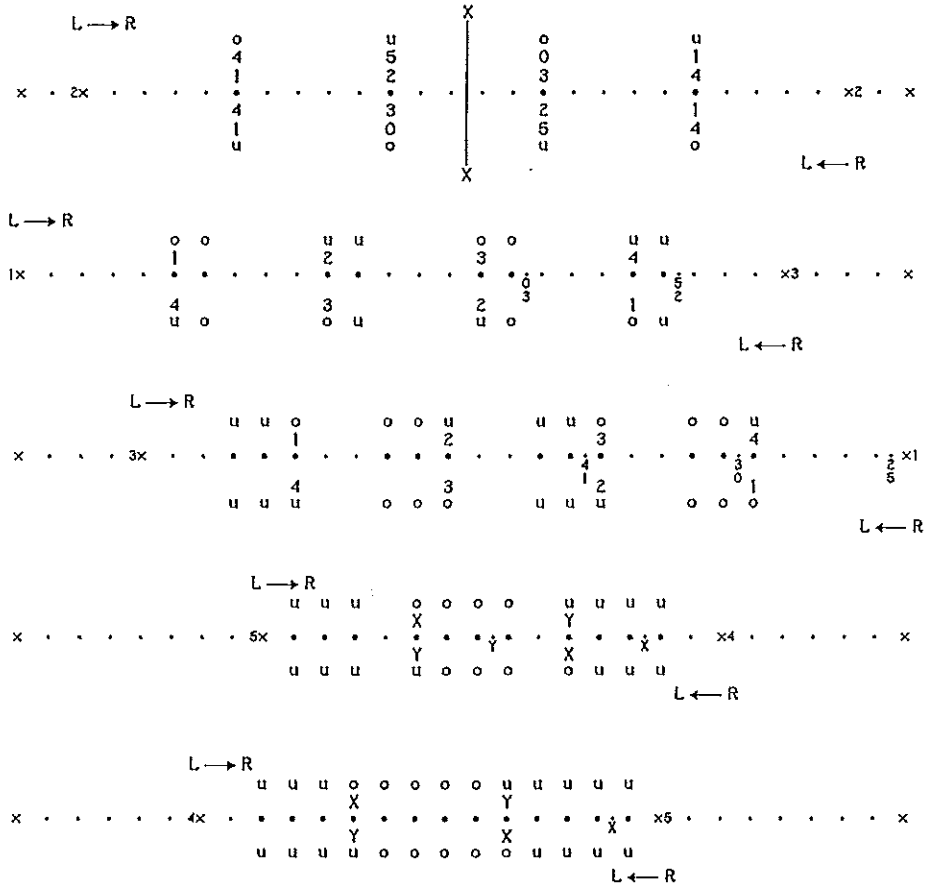

Fig. 784 — The algorithm diagrams showing all the columns between bight-boundaries $l_i = 1$ and $r_i = 1$.

The bigger dots in these algorithm diagrams indicate the actual intersection-columns associated with the component under consideration. In Fig. 784 we have the following sequence of algorithm diagrams:

The uppermost diagram is associated with the first component, the foundation knot, between left bight-boundary 2 and right bight-boundary 2. The next is associated with the second component between left bight-boundary 1 and right bight-boundary 3. The next is associated with the third component between left bight-boundary 3 and right bight-boundary 1. The next is associated with the fourth component between left bight-boundary 5 and right bight-boundary 4. And the lowermost is associated with the fifth component between left bight-boundary 4 and right bight-boundary 5.

The **over**-crossings between a lower-right to upper-left half-cycle of a component with the outgoing half-cycle parts 7 & 7′ of the foundation knot are indicated by a very small + sign and its associated small numeral for the i-value of the half-cycle concerned (readily obtainable from the string-run diagram or the grid-diagram in Fig. 783)).

Note that for the first to be braided sub-component of the components 4 and 5 the X and Y positions are neglected; for the second sub-component the bigger X and smaller X positions are to be taken into account; and for the third sub-component the positions with bigger X and Y and smaller Y when present are to be taken into account.

The Perfect and Semi-Perfect Herringbone Pineapple Knots:

First we calculate the first-return string-run with its associated nest-index numbers for braiding the knot in the normal way with its first half-cycle starting on its associated left bight-boundary (hence with its string-run not passing diametrically through the object over which it sits). For these nest-index numbers we use the formulae:†

$$I_{R_1} = I_{L_1} = 0$$
$$I_{L_{n+1}} = |I_{L_n} + 4A + x - (l_n + l_{n+1} + 2r_n)|_B$$
$$I_{R_{n+1}} = |I_{R_n} + 4A + x - (r_n + r_{n+1} + 2l_n)|_B$$

The number of crossings associated with a half-cycle are for this case calculated with the formula $2A + x - 1 - (l_n + r_n)$.‡ Then we construct the half-cycle pattern for this case and then modify the half-cycle numbers so as to comply with the string passing diametrically through the object over which the knot sits (we shall again use parallel braiding).

For the **Perfect Herringbone Pineapple Knots** the string-run consists of two equal sections starting with the half-cycle parts 1 and 1′ respectively and ending with the outgoing half-cycles $(B+1)$ and $(B+1)'$ respectively. Half-cycle $(B+1)'$ and extended half-cycle part 1 occupy the same position on the left bight-boundary l_i at nest-index number $I_{L_1} = I_{L_{(B+1)'}} = 0$, while half-cycle $(B+1)$ and extended half-cycle part 1′ occupy the same position on the left bight-boundary $\left|l_i + \frac{AB^*}{2}\right|_A$ at nest-index number $I_{L_{1'}} = I_{L_{(B+1)}} = A\left\lceil \frac{B^*}{2} - \frac{l_i - 1}{A} \right\rceil$.††

Two sequential half-cycle numbers h_n and $(h_n + 2A)$, or $(h_n)'$ and $(h_n + 2A)'$,

† See *The Braider*, Issue No. 26, pp. 592-593.

‡ See *The braider*, Issue No. 28, pg. 647.

†† $\lceil x \rceil$ denotes the smallest whole number equal to or greater than x.

where $1 \leq h_n \leq (AB^* + 1 - 2A)$, on the same bight-boundary are associated respectively with nest-index number I and nest-index number $\left|I + 2A^2 + A(x-2)\right|_B$.

For the **Semi-Perfect Herringbone Pineapple Knots** we have a number of string-run types for the foundation knot (the knot with its string diametrically through the object over which the Semi-Perfect Herringbone Pineapple sits):

Type I — Example:

Let $A = 4$; $x = 9$; $B^* = 25$; $y = A + 1 = 5$. Hence $k = \left|\frac{x-A-3}{2}\right|_A = \left|\frac{9-4-3}{2}\right|_4 = 1$, and $\Delta = |y|_A = |5|_4 = 1$. $P = 2A + x - 2 = 2\times4+9-2 = 15$, hence $\lambda = \text{g.c.d.}\,(P, B^*) = \text{g.c.d.}\,(15, 25) = 5$; each sub-component has thus $\frac{AB^*}{\lambda} = \frac{100}{5} = 20$ bights.

Let the extended half-cycle part 1 be on the bight-boundary l_i at nest-index number $I_{L_{l_i}} = 0$, and let the extended half-cycle part 1′ be on the bight-boundary $(l_i)' = \left|l_i + \frac{AB^*}{2}\right|_A$ at nest-index number $I_{L_{(l_i)'}} = \left|I_{L_{l_i}} + A\left\lceil \frac{B^*}{2} - \frac{l_i - 1}{A}\right\rceil\right|_B$.

The first-return string-run and its associated nest-index numbers are calculated in the usual manner, then for the to bight-boundary 1 extended lower-left to upper-right half-cycles the index numbers at bight-boundary 1 are calculated with the formula $I_{\text{at } l_1} = \left|I_{L_n} + 1 - l_n + mI_{L_{(A+1)}}\right|_B$, where $1 \leq n \leq A+1$ and $0 \leq m \leq \frac{B^*}{\lambda} - 1$, while $I_{L_n} = \left|I_{L_{n-1}} + 4A + x - (l_{n-1} + l_n + 2r_{n-1})\right|_B$ for $2 \leq n \leq A+1$ and with $I_{L_1} = 0$ (these index numbers are shown on the extreme left of the first-return string-run). Hence $\left|I_{L_{(l_i)'}} - I_{L_{l_i}} + l_i - (l_i)'\right|_B = \frac{AB^*}{2} = \frac{B}{2} = \frac{100}{2} = 50$.

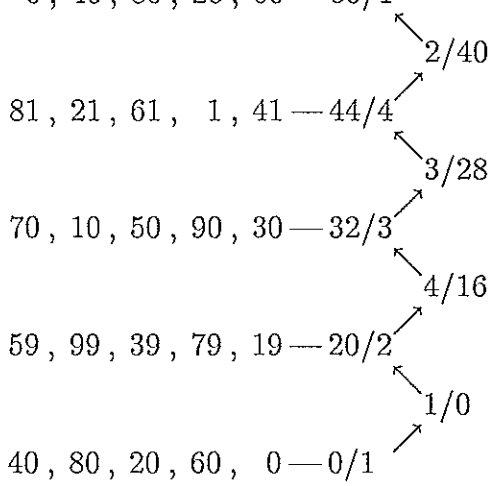

$I_{L_1} = 0$.

$I_{L_2} = |I_{L_1} + 4A + x - (l_1 + l_2 + 2r_1)|_B = |0 + 4\times4 + 9 - (1 + 2 + 2\times1)|_{100} = 20$.

$I_{L_3} = |I_{L_2} + 4A + x - (l_2 + l_3 + 2r_2)|_B = |20 + 4\times4 + 9 - (2 + 3 + 2\times4)|_{100} = 32$.

$I_{L_4} = |I_{L_3} + 4A + x - (l_3 + l_4 + 2r_3)|_B = |32 + 4\times4 + 9 - (3 + 4 + 2\times3)|_{100} = 44$.

$I_{L_5} = |I_{L_4} + 4A + x - (l_4 + l_5 + 2r_4)|_B = |44 + 4\times4 + 9 - (4 + 1 + 2\times2)|_{100} = 60$.

$I_{R_1} = 0$.

$I_{R_2} = |I_{R_1} + 4A + x - (r_1 + r_2 + 2l_2)|_B = |0 + 4\times4 + 9 - (1 + 4 + 2\times2)|_{100} = 16$.

$I_{R_3} = |I_{R_2} + 4A + x - (r_2 + r_3 + 2l_3)|_B = |16 + 4\times4 + 9 - (4 + 3 + 2\times3)|_{100} = 28$.

$I_{R_4} = |I_{R_3} + 4A + x - (r_3 + r_4 + 2l_4)|_B = |28 + 4\times4 + 9 - (3 + 2 + 2\times4)|_{100} = 40$.

From the index numbers at the extreme left of the first-return string-run we see that $\left|I_{L_{(l_i)'}} - I_{L_{l_i}} + l_i - (l_i)'\right|_B = 50$ for $l_i = 1$ at nest-index number $I_{L_1} = 0$ and $(l_i)' = 3$ at nest-index number $I_{L_3} = 52$. Thus half-cycle part 1 can be associated with the lower-left to upper-right half-cycle starting on left bight-boundary 1 at nest-index number 0, and half-cycle part 1′ can be associated with the lower-left to upper-right half-cycle starting on left bight-boundary 3 at nest-index number 52. Since this involves the string-run of one sub-component with 20 bights, the outgoing lower-left to upper-right half-cycles are 21 'coinciding' with half-cycle part 1′, and 21′ 'coinciding'

with half-cycle part 1. In Fig. 785 a part of the string-run of the foundation knot is shown. Note the lengthways offset position for the diametrical string passage of the foundation knot due to the small x-value.

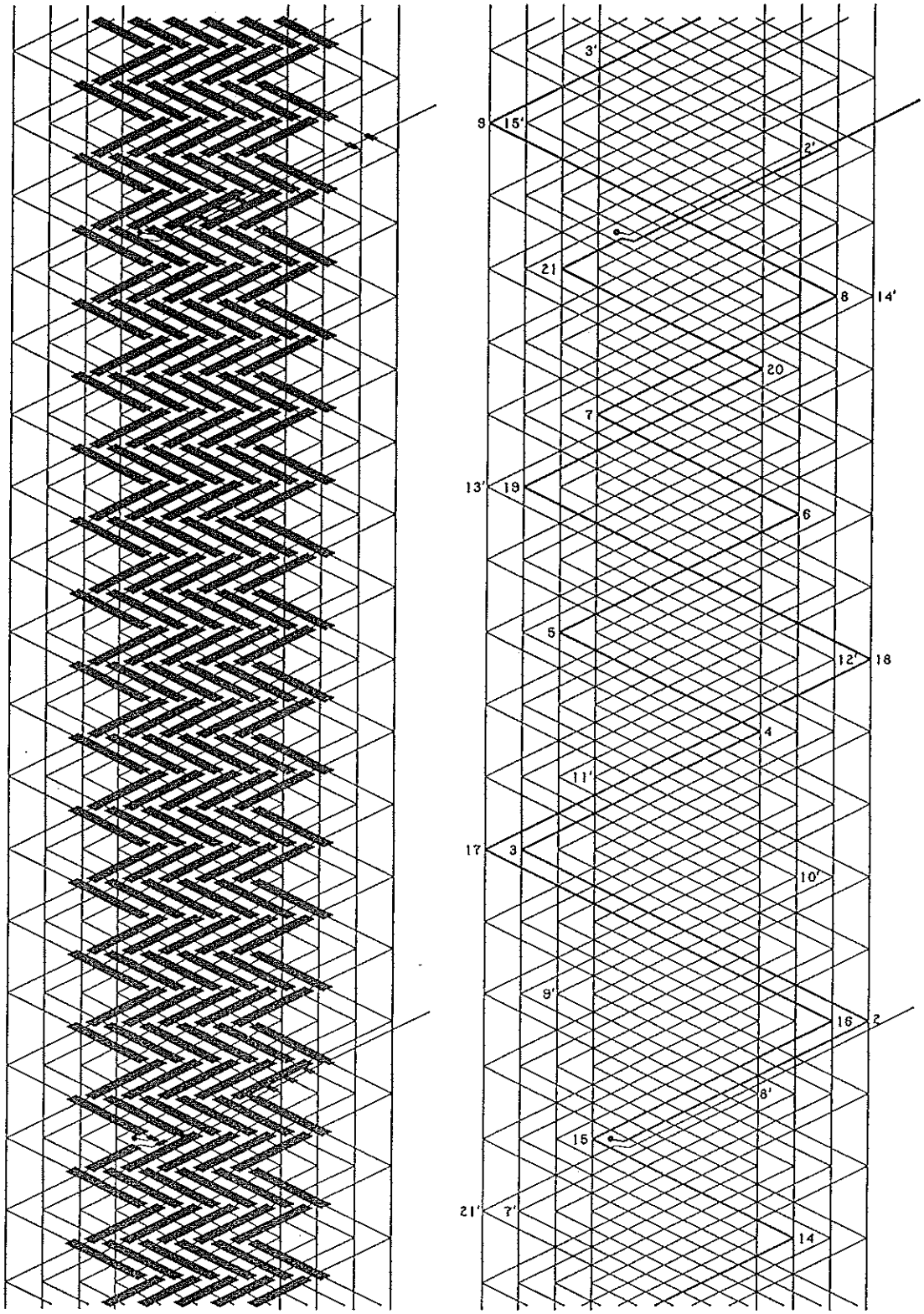

Fig. 785 — Part of grid-diagram and string-run diagram.

For greater x-values a more balanced position for the diametrical string passage of the foundation knot can be achieved (see for example Fig.thinspace786 where $x = 29$ and $B^* = 15$).

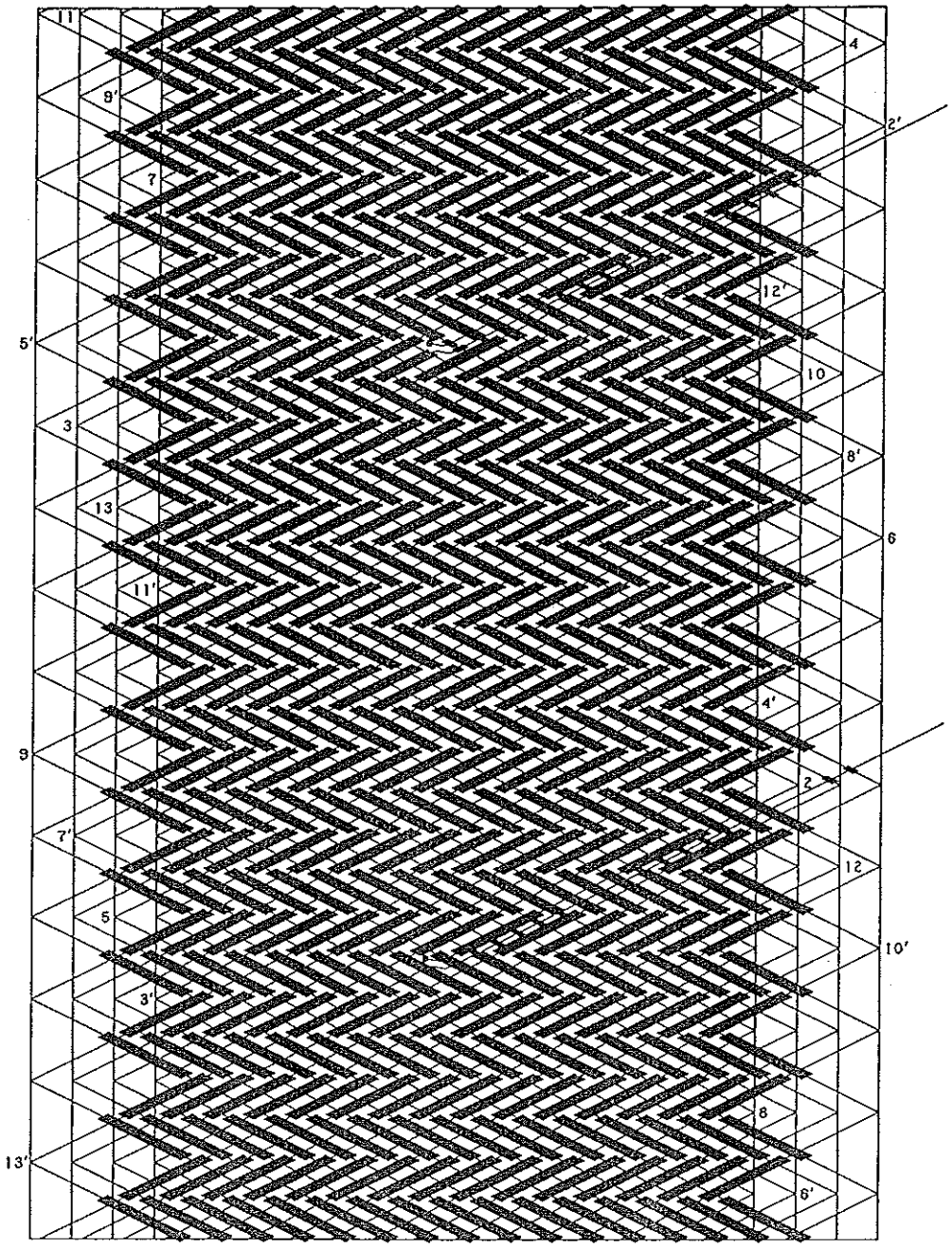

Fig. 786 — $A = 4$; $x = 29$; $y = A + 1 = 5$; $B^* = 15$. Hence $k = 3$ and $\Delta = 1$.

Type II — Example :

Let $A = 4$; $x = 19$; $B^* = 15$; $y = A + 1 = 5$. Hence $k = \left|\frac{x-A-3}{2}\right|_A = \left|\frac{19-4-3}{2}\right|_4 = 2$, and $\Delta = |y|_A = |5|_4 = 1$. $P = 2A + x - 2 = 2 \times 4 + 19 - 2 = 25$, hence $\lambda = \text{g.c.d.}(P, B^*) = \text{g.c.d.}(25, 15) = 5$; each sub-component has thus $\frac{AB^*}{\lambda} = \frac{60}{5} = 12$ bights.

Let the extended half-cycle part 1 be on the bight-boundary l_i at nest-index number $I_{L_{l_i}} = 0$, and let the extended half-cycle part $1'$ be on the bight-boundary $(l_i)' = \left|l_i + \frac{AB^*}{2}\right|_A$ at nest-index number $I_{L_{(l_i)'}} = \left|I_{L_{l_i}} + A\left\lceil\frac{B^*}{2} - \frac{l_i - 1}{A}\right\rceil\right|_B$.

The first-return string-run and its associated nest-index numbers are calculated in the usual manner, then for the to bight-boundary 1 extended lower-left to upper-right

half-cycles the index numbers at bight-boundary 1 are calculated with the formula $I_{\text{at } l_1} = \left|I_{L_n} + 1 - l_n + mI_{L_{(A+1)}}\right|_B$, where $1 \leq n \leq A+1$ and $0 \leq m \leq \frac{B^*}{\lambda} - 1$, while $I_{L_n} = \left|I_{L_{n-1}} + 4A + x - (l_{n-1} + l_n + 2r_{n-1})\right|_B$ for $2 \leq n \leq A+1$ and with $I_{L_1} = 0$ (these index numbers are shown on the extreme left of the first-return string-run). Hence $\left|I_{L_{(l_i)'}} - I_{L_{l_i}} + l_i - (l_i)'\right|_B = \frac{AB^*}{2} = \frac{B}{2} = \frac{60}{2} = 30$.

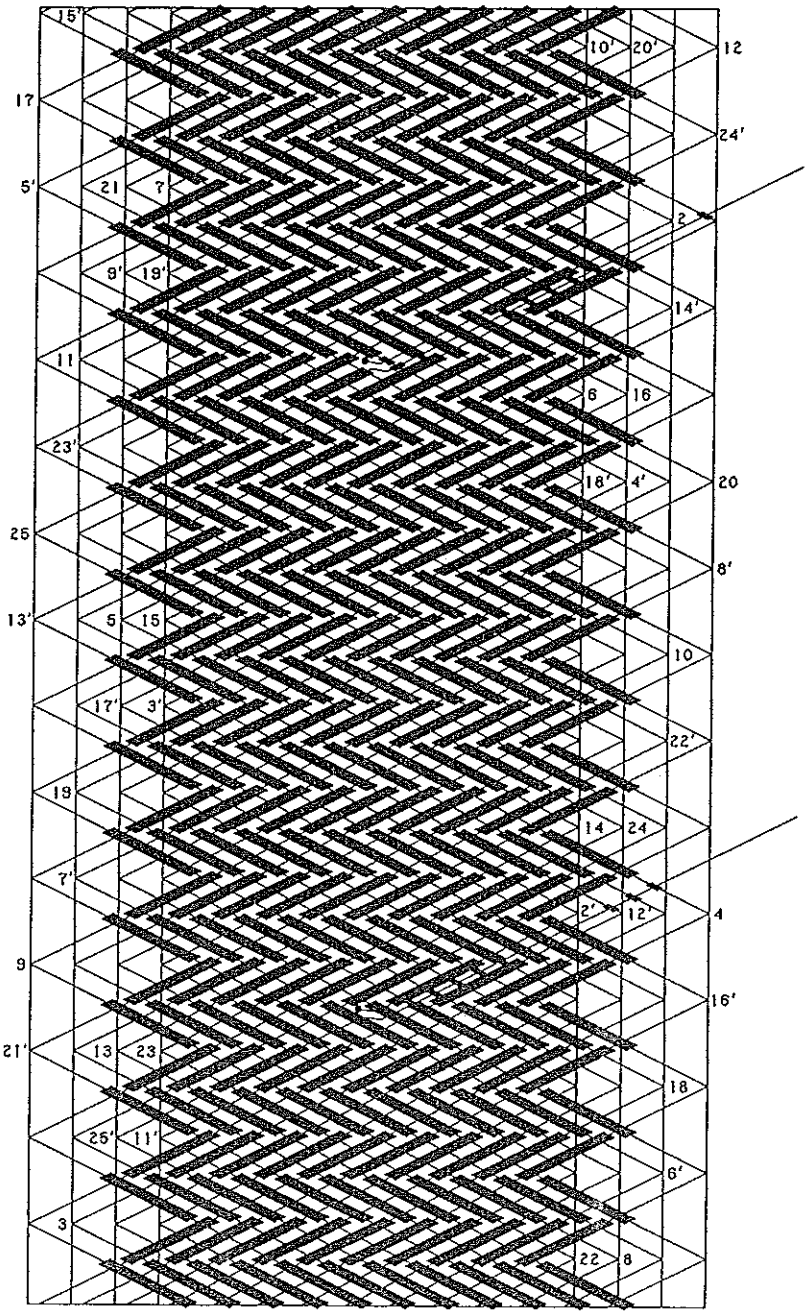

Fig. 787 — $A = 4$; $x = 19$; $y = A + 1 = 5$; $B^* = 15$. Hence $k = 2$ and $\Delta = 1$.

The index numbers at the extreme left of the first-return string-run clearly show that there isn't an l_i and $(l_i)'$, belonging to the same sub-component, for which $\left|I_{L_{(l_i)'}} - I_{L_{l_i}} + l_i - (l_i)'\right|_B = 30$. The grid-diagram (see Fig. 787) shows that we can place the string, which runs diametrically through the object over which the Semi-Perfect Herringbone Pineapple sits, between the lower-left to upper-right half-cycles

which start on left bight-boundary $l_i = 1$ at $I_{L_{l_i}} = 0$ and on left bight-boundary $(l_i)' = 3$ at $I_{L_{(l_i)'}} = 32$. Note that the diametrically through string joins two sub-components, and hence the outgoing half-cycles are $\frac{2AB^*}{\lambda} + 1 = 25$ and $(\frac{2AB^*}{\lambda} + 1)' = 25'$ which respectively 'coincide' with half-cycle parts 1 and 1′.

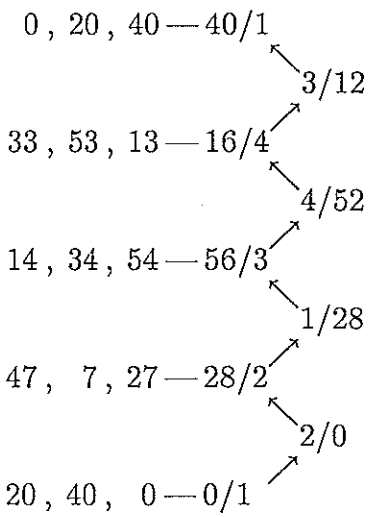

$$
\begin{aligned}
I_{L_1} &= 0 .\\
I_{L_2} &= |I_{L_1} + 4A + x - (l_1 + l_2 + 2r_1)|_B = \\
&\quad |0 + 4 \times 4 + 19 - (1 + 2 + 2 \times 2)|_{60} = 28 .\\
I_{L_3} &= |I_{L_2} + 4A + x - (l_2 + l_3 + 2r_2)|_B = \\
&\quad |28 + 4 \times 4 + 19 - (2 + 3 + 2 \times 1)|_{60} = 56 .\\
I_{L_4} &= |I_{L_3} + 4A + x - (l_3 + l_4 + 2r_3)|_B = \\
&\quad |56 + 4 \times 4 + 19 - (3 + 4 + 2 \times 4)|_{60} = 16 .\\
I_{L_5} &= |I_{L_4} + 4A + x - (l_4 + l_5 + 2r_4)|_B = \\
&\quad |16 + 4 \times 4 + 19 - (4 + 1 + 2 \times 3)|_{60} = 40 .\\
I_{R_1} &= 0 .\\
I_{R_2} &= |I_{R_1} + 4A + x - (r_1 + r_2 + 2l_2)|_B = \\
&\quad |0 + 4 \times 4 + 19 - (2 + 1 + 2 \times 2)|_{60} = 28 .\\
I_{R_3} &= |I_{R_2} + 4A + x - (r_2 + r_3 + 2l_3)|_B = \\
&\quad |28 + 4 \times 4 + 19 - (1 + 4 + 2 \times 3)|_{60} = 52 .\\
I_{R_4} &= |I_{R_3} + 4A + x - (r_3 + r_4 + 2l_4)|_B = \\
&\quad |52 + 4 \times 4 + 19 - (4 + 3 + 2 \times 4)|_{60} = 12 .
\end{aligned}
$$

Type III — Example:

Let $A = 4$; $x = 19$; $B^* = 10$; $y = A + 1 = 5$. Hence $k = \left|\frac{x-A-3}{2}\right|_A = \left|\frac{19-4-3}{2}\right|_4 = 2$, and $\Delta = |y|_A = |5|_4 = 1$. $P = 2A + x - 2 = 2 \times 4 + 19 - 2 = 25$, hence $\lambda = \text{g.c.d.}(P, B^*) = \text{g.c.d.}(25, 10) = 5$; each sub-component has thus $\frac{AB^*}{\lambda} = \frac{40}{5} = 8$ bights.

Let the extended half-cycle part 1 be on the bight-boundary l_i at nest-index number $I_{L_{l_i}} = 0$, and let the extended half-cycle part 1′ be on the bight-boundary $(l_i)' = \left|l_i + \frac{AB^*}{2}\right|_A$ at nest-index number $I_{L_{(l_i)'}} = \left|I_{L_{l_i}} + A\left\lceil \frac{B^*}{2} - \frac{l_i - 1}{A}\right\rceil\right|_B$.

The first-return string-run and its associated nest-index numbers are calculated in the usual manner, then for the to bight-boundary 1 extended lower-left to upper-right half-cycles the index numbers at bight-boundary 1 are calculated with the formula $I_{\text{at } l_1} = \left|I_{L_n} + 1 - l_n + mI_{L_{(A+1)}}\right|_B$, where $1 \le n \le A + 1$ and $0 \le m \le \frac{B^*}{\lambda} - 1$, while $I_{L_n} = \left|I_{L_{n-1}} + 4A + x - (l_{n-1} + l_n + 2r_{n-1})\right|_B$ for $2 \le n \le A + 1$ and with $I_{L_1} = 0$ (these index numbers are shown on the extreme left of the first-return string-run). Hence $\left|I_{L_{(l_i)'}} - I_{L_{l_i}} + l_i - (l_i)'\right|_B = \frac{AB^*}{2} = \frac{B}{2} = \frac{40}{2} = 20$.

From the index numbers at the extreme left of the first-return string-run we see that $\left|I_{L_{(l_i)'}} - I_{L_{l_i}} + l_i - (l_i)'\right|_B = \frac{AB^*}{2} = \frac{B}{2} = \frac{40}{2} = 20$. For $(l_i)' = l_i$ with l_i at $I_{L_{l_i}} = 0$ and $(l_i)'$ at $I_{L'_{(l_i)}} = 20$

Thus half-cycle part 1 can be associated with the lower-left to upper-right half-cycle starting on left bight-boundary 3 at nest-index number 0, and half-cycle part 1′ can be associated with the lower-left to upper-right half-cycle starting on left bight-boundary 3 at nest-index number 20. Since this involves the string-run of one sub-component with

$\frac{B}{\lambda} = \frac{40}{5} = 8$ bights, the outgoing lower-left to upper-right half-cycles are $9'$ 'coinciding' with half-cycle part 1, and 9 'coinciding' with half-cycle part $1'$.

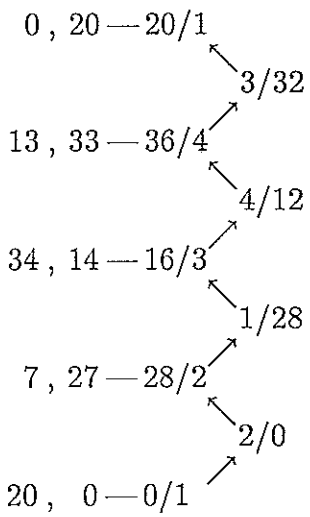

$$I_{L_1} = 0.$$
$$I_{L_2} = |I_{L_1} + 4A + x - (l_1 + l_2 + 2r_1)|_B = |0 + 4 \times 4 + 19 - (1 + 2 + 2 \times 2)|_{40} = 28.$$
$$I_{L_3} = |I_{L_2} + 4A + x - (l_2 + l_3 + 2r_2)|_B = |28 + 4 \times 4 + 19 - (2 + 3 + 2 \times 1)|_{40} = 16.$$
$$I_{L_4} = |I_{L_3} + 4A + x - (l_3 + l_4 + 2r_3)|_B = |16 + 4 \times 4 + 19 - (3 + 4 + 2 \times 4)|_{40} = 36.$$
$$I_{L_5} = |I_{L_4} + 4A + x - (l_4 + l_5 + 2r_4)|_B = |36 + 4 \times 4 + 19 - (4 + 1 + 2 \times 3)|_{40} = 20.$$
$$I_{R_1} = 0.$$
$$I_{R_2} = |I_{R_1} + 4A + x - (r_1 + r_2 + 2l_2)|_B = |0 + 4 \times 4 + 19 - (2 + 1 + 2 \times 2)|_{40} = 28.$$
$$I_{R_3} = |I_{R_2} + 4A + x - (r_2 + r_3 + 2l_3)|_B = |28 + 4 \times 4 + 19 - (1 + 4 + 2 \times 3)|_{40} = 12.$$
$$I_{R_4} = |I_{R_3} + 4A + x - (r_3 + r_4 + 2l_4)|_B = |12 + 4 \times 4 + 19 - (4 + 3 + 2 \times 4)|_{40} = 32.$$

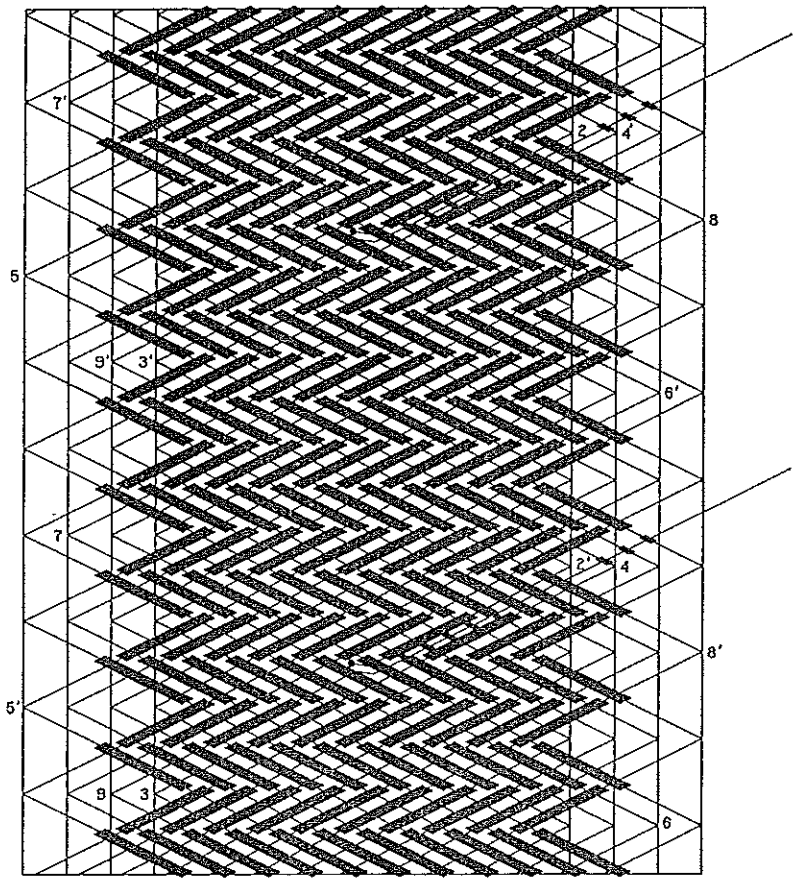

Fig. 788 — $A = 4$; $x = 19$; $y = A + 1 = 5$; $B^* = 10$. Hence $k = 2$ and $\Delta = 1$.

Besides these three string-run types I, II and III for the foundation knot, we have string-run types where the string-run from the diametrical passage position 1 describes a right helix while the string-run from the diametrical passage position $1'$ describes a left helix, or vice versa.

Example 3.

Fig. 785 shows the grid-diagram of a 2-pass Perfect Herringbone Pineapple Knot (hence $A = 2$), with its string passing diametrically through the object which it encircles. The further particulars of this knot are $x = 9$, $y = A - 1 = 1$, $B^* = 5$. Hence $k = \left|\frac{x-A-1}{2}\right|_A = \left|\frac{9-2-1}{2}\right|_2 = |3|_2 = 1$ and $\Delta = |y|_A = |1|_2 = 1$.

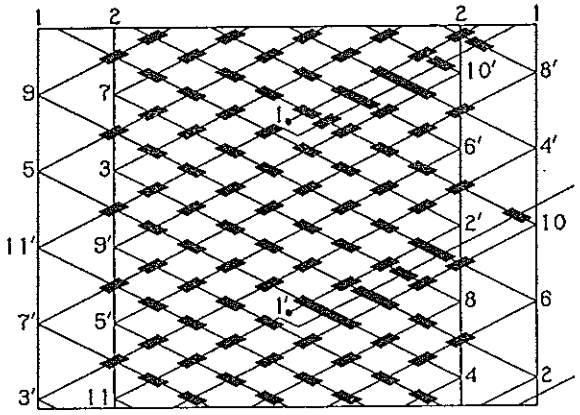

Fig. 789 — The Perfect Herringbone Pineapple Knot with $A = 2$, $x = 9$, $B^* = 5$, $y = A - 1$.

Hence in our Example with half-cycle $(B+1)' = 11'$ and extended half-cycle part 1 starting on left bight-boundary $l_i = 1$ at nest-index number $I_{L_1} = I_{L_{(B+1)'}} = I_{L_{11'}} = 0$, half-cycle $(B+1) = 11$ and extended half-cycle part $1'$ start on left bight-boundary $\left|l_i + \frac{AB^*}{2}\right|_A = \left|1 + \frac{10}{2}\right|_2 = 2$ at nest-index number $I_{L_{1'}} = I_{L_{(B+1)}} = I_{L_{11}} = A\left\lceil \frac{B^*}{2} - \frac{l_i - 1}{A} \right\rceil = 2\left\lceil \frac{5}{2} - \frac{1-1}{2} \right\rceil = 2 \times 3 = 6$.

Hence for our Example here we obtain the first-return string-run and half-cycle pattern shown in Fig. 790.

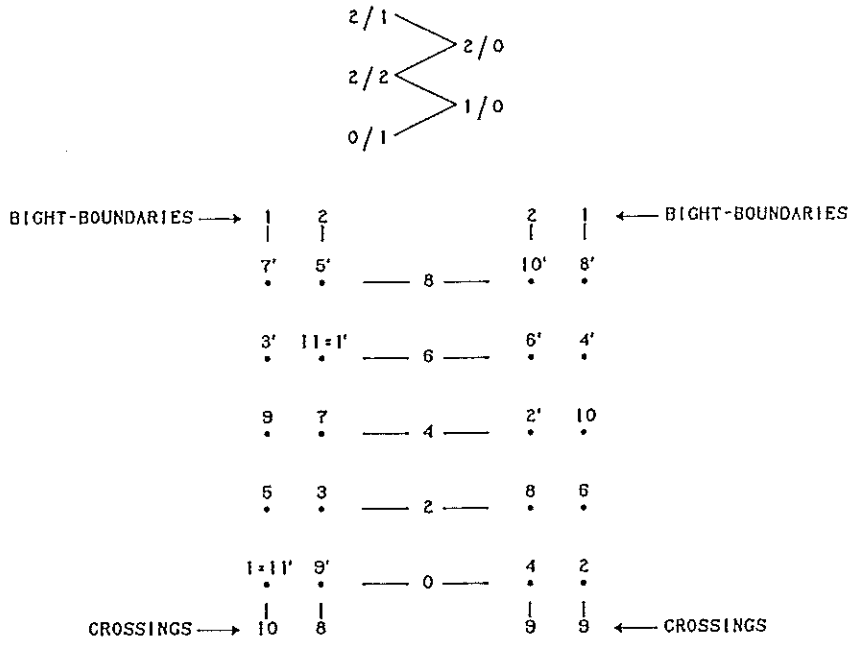

Fig. 790 — First-return string-run and half-cycle pattern for Example 3.

From the half-cycle pattern in Fig. 790 we assemble the half-cycle tables in Fig. 791.

In the odd-numbered half-cycle table the outgoing half-cycle $11'$ has two **unders** to the right of the heavy line in the penultimate bottom row. The outgoing half-cycle 11 has four **unders** to the right of the heavy line in the bottom row. In the even-numbered half-cycle tables neglect the crossed 2 and $2'$ and for half-cycle $2'$ neglect 2.

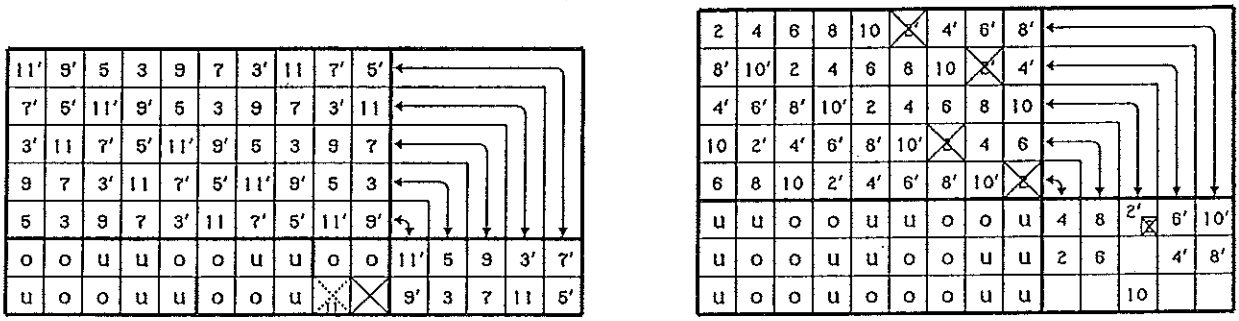

Fig. 791 — The half-cycle tables for Example 3.

From the half-cycle tables in Fig. 791 we read the half-cycle braiding algorithms:

1. $\longrightarrow 1$: Free run.
$1'$. $\longrightarrow 2$: Free run.
2. $2 \longleftarrow 1$: u.
$2'$. $1 \longleftarrow 2$: Free run.
3. $2 \longrightarrow 2$: o.
$3'$. $1 \longrightarrow 1$: $2o$.
4. $1 \longleftarrow 2$: $o - u$.
$4'$. $2 \longleftarrow 1$: $o - 2u$.
5. $1 \longrightarrow 1$: $u - 3o$.
$5'$. $2 \longrightarrow 2$: $o - u - o$.
6. $2 \longleftarrow 1$: $2o - 3u$.
$6'$. $1 \longleftarrow 2$: $2o - 2u$.
7. $2 \longrightarrow 2$: $u - o - u - o - u$.
$7'$. $1 \longrightarrow 1$: $2u - o - u - 2o$.
8. $1 \longleftarrow 2$: $u - 2o - u - o - u$.
$8'$. $2 \longleftarrow 1$: $u - 2o - u - o - 2u$.
9. $1 \longrightarrow 1$: $o - 2u - o - 2u - 2o$.
$9'$. $2 \longrightarrow 2$: $u - 2o - 2u - o - u$.
10. $2 \longleftarrow 1$: $u - 2o - u - 3o - 2u$.
$10'$. $1 \longleftarrow 2$: $2u - 2o - u - 2o - u$.
11. $2 \longrightarrow$: $u - 2o - 6u$.
$11'$. $1 \longrightarrow$: $2o - 2u - 2o - 4u$.

Example 4.

Fig. 792 shows the grid-diagram of a 5-pass Semi-Perfect Herringbone Pineapple Knot (hence $A = 5$), with its string passing diametrically through the object over which it sits. The further particulars of this knot are $x = 14$, $y = A + 1 = 6$, $B^* = 4$. Hence $k = \left|\frac{x-A-3}{2}\right|_A = \left|\frac{14-5-3}{2}\right|_5 = |3|_5 = 3$; $P = 2A + x - 2 = 10 + 14 - 2 = 22$ and $\Delta = |y|_A = |6|_5 = 1$. The number of sub-components λ is equal to g.c.d.(P, B^*) = g.c.d.$(22, 4) = 2$, hence each sub-component has $\frac{B}{\lambda} = \frac{20}{2} = 10$ bights.†

† Compare this Example with Example 4 in *The Braider*, Issue No. 29.

Hence in our Example with half-cycle $(\frac{B}{\lambda}+1)' = 11'$ and extended half-cycle part 1 starting on left bight-boundary $l_i = 1$ at nest-index number $I_{L_1} = I_{L_{(\frac{B}{\lambda}+1)'}} = I_{L_{11'}} = 0$, half-cycle $(\frac{B}{\lambda}+1) = 11$ and extended half-cycle part $1'$ start on left bight-boundary $\left|l_i + \frac{AB^*}{2}\right|_A = \left|1 + \frac{20}{2}\right|_5 = 1$ at nest-index number $I_{L_{1'}} = I_{L_{(\frac{B}{\lambda}+1)}} = I_{L_{11}} = A\left\lceil \frac{B^*}{2} - \frac{l_i - 1}{A}\right\rceil = 5\left\lceil \frac{4}{2} - \frac{1-1}{2}\right\rceil = 5 \times 2 = 10$.

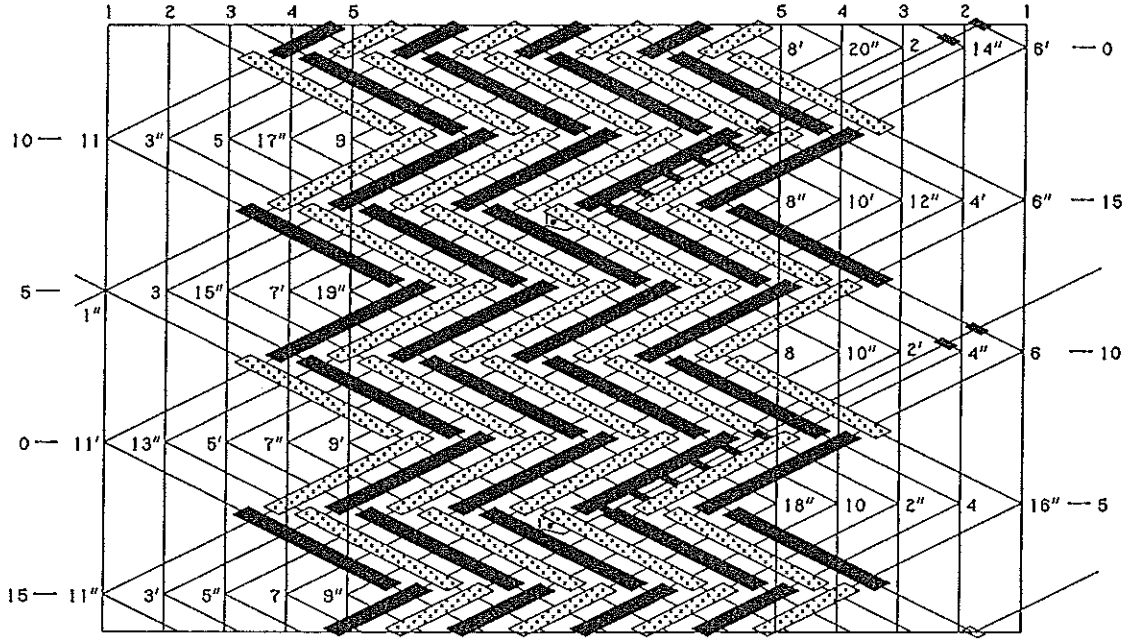

Fig. 792 — The 5-pass Semi-Perfect Herringbone Pineapple Knot of Example 4. Its first-return string-run and half-cycle pattern are depicted in Fig. 793.

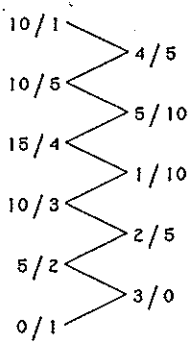

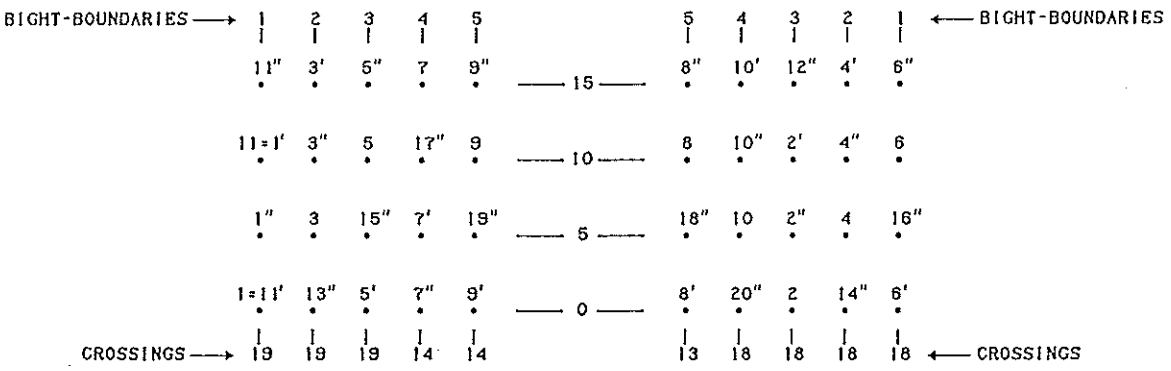

Fig. 793 — First-return string-run and half-cycle pattern.

From the half-cycle pattern in Fig. 793 and the grid-diagram in Fig. 792 we assemble the half-cycle tables in Fig. 794. In the upper table (for the odd-numbered half-cycles from lower-left to upper-right) the codings to the right of the short heavy vertical line segment are **unders** for the half-cycles 11 and $11'$, while for the $''$ half-cycles the crossed-out $1''$ boxes are to be neglected. In the lower table (for the even-numbered half-cycles from lower-right to upper-left) the $2_\star$ and $2'_\star$ boxes are to be neglected for the half-cycles $2_\star$, $2'_\star$, $4_\star$, $4'_\star$, $6_\star$, $6'_\star$, $8_\star$, $8'_\star$, $10_\star$ and $10'_\star$, while the $_\star 2$ and $_\star 2'$ boxes are to be neglected for the half-cycles $_\star 8$ and $_\star 8'$. For the relevant even-numbered $''$ half-cycles the heavy lined boxes 2, $2'$, $_\star 2$ and $_\star 2'$ are associated with the indicated coding preceded by o.

L ⟶ R

11'	13"	5'	7"	9'	⊠	3	15"	7'	19"	11	3"	5	17"	9	11"	3'	5"	7					
11"	3'	5"	7	9"	11'	13"	5'	7"	9'	⊠	3	15"	7'	19"	11	3"	5	17"	7				
11	3"	5	17"	9	11"	3'	5"	7	9"	11'	13"	5'	7"	9'	⊠	3	15"	7'					
⊠	3	15"	7'	19"	11	3"	5	17"	9	11"	3'	5"	7	9"	11'	13"	5'	7"	7'				
u	o	o	o	o	o	u	u	u	u	u	o	o	o	o	o	u	u	u	u	11'	1"	11	11"
u	u	o	o	o	o	o	u	u	u	u	u	o	o	o	o	o	u	u		13"	3	3"	3'
u	u	u	o	o	o	o	o	u	u	u	u	u	o	o	o	o	o	u		5'	15"	5	5"
u	u	u	u	o	o	o	o	o	u	u	u	u	u							7"	7'	17"	7
u	u	u	u	u	o	o	o	o	o	u	u	u	u							9'	19"	9	9"

R ⟶ L

	6'	14"	2	20"	8'	16"	4	2"	10	18"	6	4"	$2'_\star$	10"	8	6"	4'	12"					
2'	6"	4'	12"	10'	8"	6'	14"	$_\star 2$	20"	8'	16"	4	2"	10	18"	6	4"	$2'_\star$					
	6	4"	2'	10"	8	6"	4'	12"	10'	8"	6'	14"	$2_\star$	20"	8'	16"	4	2"					
2	16"	4	2"	10	18"	6	4"	$_\star 2'$	10"	8	6"	4'	12"	10'	8"	6'	14"	$2_\star$					
	o	o	o	o	o	u	u	u	u	u	o	o	o	o	o	u	u	u	$6'_\star$	$16"_\star$	$6_\star$	$6"_\star$
o	u	o	o	o	o	o	u	u	u	u	u	o	o	o	o	o	u	u	$14"_\star$	$4_\star$	$4"_\star$	$4'_\star$	
	u	u	o	o	o	o	o	u	u	u	u	u	o	o	o	o	o	u	$2_\star$	$2"_\star$	$2'_\star$	$12"_\star$	
	u	u	u	o	o	o	o	o	u	u	u	u	u	o	o	o	o	o	$20"_\star$	$10_\star$	$10"_\star$	$10'_\star$	
	u	u	u	u	o	o	o	o	o	u	u	u	u						$8'_\star$	$18"_\star$	$8_\star$	$8"_\star$	

Fig. 794 — The half-cycle tables for Example 4.

The half-cycle tables in Fig. 794 supply the following half-cycle braiding algorithms:

half-cycle part 1	$\longrightarrow 3 = r_i$	:	Free run.
half-cycle part $1'$	$\longrightarrow 3 = r_i$	:	Free run.
half-cycle 2	$l_i = 2 \longleftarrow 3 = r_i$	:	u.
half-cycle $2'$	$l_i = 2 \longleftarrow 3 = r_i$	:	u.
half-cycle 3	$l_i = 2 \longrightarrow 2 = r_i$	:	$2o$.
half-cycle $3'$	$l_i = 2 \longrightarrow 2 = r_i$	:	$2o$.
half-cycle 4	$l_i = 3 \longleftarrow 2 = r_i$	:	$o - 2u$.
half-cycle $4'$	$l_i = 3 \longleftarrow 2 = r_i$	:	$o - 2u$.
half-cycle 5	$l_i = 3 \longrightarrow 1 = r_i$	:	$u - o - u - o$.
half-cycle $5'$	$l_i = 3 \longrightarrow 1 = r_i$	:	$u - o - u - o$.
half-cycle 6	$l_i = 4 \longleftarrow 1 = r_i$	:	$o - 2u - o - u$.
half-cycle $6'$	$l_i = 4 \longleftarrow 1 = r_i$	:	$o - 2u - o - u$.
half-cycle 7	$l_i = 4 \longrightarrow 5 = r_i$	:	$u - 2o - u$.
half-cycle $7'$	$l_i = 4 \longrightarrow 5 = r_i$	:	$u - 2o - u$.
half-cycle 8	$l_i = 5 \longleftarrow 5 = r_i$	:	$u - o - 2u$.
half-cycle $8'$	$l_i = 5 \longleftarrow 5 = r_i$	:	$u - o - 2u$.

half-cycle 9	$l_i = 5 \longrightarrow 4 = r_i$	:	$2u - 2o - 2u$.
half-cycle 9′	$l_i = 5 \longrightarrow 4 = r_i$	:	$2u - 2o - 2u$.
half-cycle 10	$l_i = 1 \longleftarrow 4 = r_i$	:	$2u - 2o - 2u - 2o$.
half-cycle 10′	$l_i = 1 \longleftarrow 4 = r_i$	:	$2u - 2o - 2u - 2o$.
half-cycle 11	$l_i = 1 \longrightarrow$	:	$3o - 7u$.
half-cycle 11′	$l_i = 1 \longrightarrow$	:	$3o - 7u$.

.....

half-cycle 1″	$l_i = 1 \longrightarrow 3 = r_i$	:	$u - 2o - 3u - 2o - 2u$.
half-cycle 2″	$l_i = 2 \longleftarrow 3 = r_i$	:	$u - 4o - 2u - 3o - u$.
half-cycle 3″	$l_i = 2 \longrightarrow 2 = r_i$	:	$u - 2o - 3u - 3o - u$.
half-cycle 4″	$l_i = 3 \longleftarrow 2 = r_i$	:	$5o - 2u - 4o - u$.
half-cycle 5″	$l_i = 3 \longrightarrow 1 = r_i$	:	$2u - 2o - 4u - 3o - u$.
half-cycle 6″	$l_i = 4 \longleftarrow 1 = r_i$	:	$4o - 3u - 4o - 2u$.
half-cycle 7″	$l_i = 4 \longrightarrow 5 = r_i$	:	$2u - 3o - 4u$.
half-cycle 8″	$l_i = 5 \longleftarrow 5 = r_i$	:	$u - o - u - 4o - 3u$.
half-cycle 9″	$l_i = 5 \longrightarrow 4 = r_i$	:	$4u - 2o - 3u$.
half-cycle 10″	$l_i = 1 \longleftarrow 4 = r_i$	:	$2u - 5o - 3u - 4o$.
half-cycle 11″	$l_i = 1 \longrightarrow 3 = r_i$	:	$u - 3o - 3u - 4o - 3u$.
half-cycle 12″	$l_i = 2 \longleftarrow 3 = r_i$	:	$u - 4o - 4u - 5o - u$.
half-cycle 13″	$l_i = 2 \longrightarrow 2 = r_i$	:	$u - 3o - 4u - 5o - 2u$.
half-cycle 14″	$l_i = 3 \longleftarrow 2 = r_i$	:	$5o - u - o - 4u - 5o - 2u$.
half-cycle 15″	$l_i = 3 \longrightarrow 1 = r_i$	:	$3u - 4o - 5u - 4o - u$.
half-cycle 16″	$l_i = 4 \longleftarrow 1 = r_i$	:	$6o - 5u - 4o - 3u$.
half-cycle 17″	$l_i = 4 \longrightarrow 5 = r_i$	:	$4u - 5o - 4u$.
half-cycle 18″	$l_i = 5 \longleftarrow 5 = r_i$	:	$2u - o - 2u - 5o - 4u$.
half-cycle 19″	$l_i = 5 \longrightarrow 4 = r_i$	:	$5u - 5o - 4u$.
half-cycle 20″	$l_i = 1 \longleftarrow 4 = r_i$	:	$3u - 6o - 5u - 5o$.

Braid Design

We have met, in previous issues of *The Braider*, the 'conventional' grid-diagrams for depicting **round braids**. They had the advantage in clearly showing the actual braid-pattern of the round braid and hence are the normally employed grid-diagrams for these braids. However, a round braid can also be depicted by another type of grid-diagram — the **UT-OT grid-diagram** (UT = under turn, OT = over turn). Those readers who are in the possession of our Pamphlet No. 1 (published in January 1991) have already met this type of diagram which depicts **the braiding** of a **round braid** in the manner of a **flat braid**. Such a flat-braided round braid can be either kept and used in its flat-braided form or kept and used as a normal round braid. When it is kept and used in its flat-braided form we shall group it under the **flat tubular braids**, and call it a **primitive flat tubular braid**. Thus note that a **primitive flat tubular braid** is in essence a **round braid**, but that a **round braid** is **not** a **primitive flat tubular braid**.

These **primitive flat tubular braids** provide us with an opportunity to design a vast range of really beautiful 'new' braids. We shall start with a few very simple examples:

On the far right in Fig. 795 is depicted the conventional grid-diagram of an under-over coded 6-lead round braid and on the far left is depicted one of its two pictorial UT-OT diagram forms (depicted is the form where a 'half-cycle' of a front-facing string of a left helix (hence from upper-left to lower-right) starts at the left with an under; the other form starts at the left with an over). The UT-OT grid-diagram associated with this UT-OT pictorial diagram is shown by the central diagram. Note that every under-over coded round braid has two different UT-OT grid-diagrams.

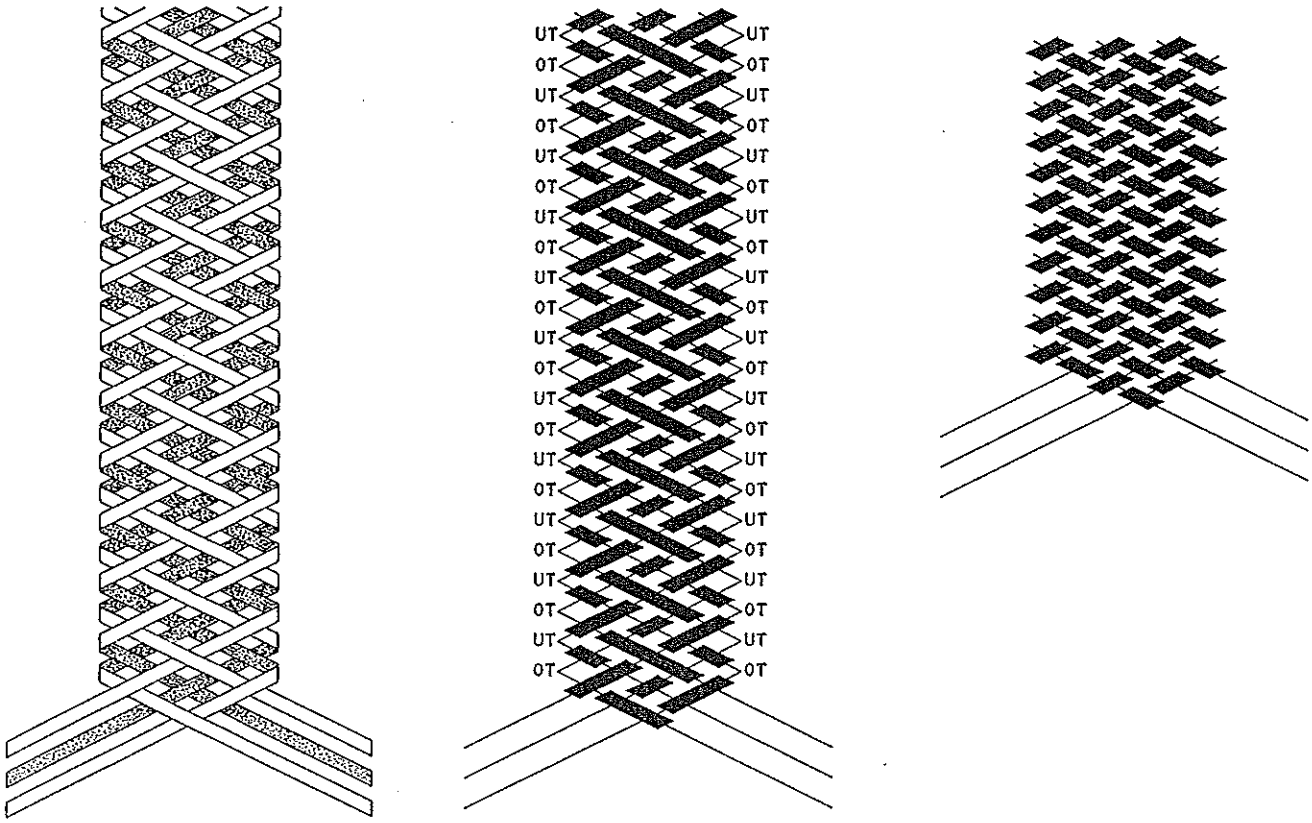

Fig. 795 — An UT-OT grid-diagram of a 6-lead under-over coded round braid.

In the upper-left pictorial diagram of Fig. 796 two of these in Fig. 795 pictorial UT-OT braids (shown again at the upper-right in Fig. 796) are placed side by side as indicated. All the right UT's and OT's of the left UT-OT braid and all the left UT's and OT's of the right UT-OT braid are cut and the cut-ends of their front-facing strings are joined and so are the cut-ends of their back-facing strings, while ensuring that at these joints the front-facing strings run behind the back-facing strings. The result of this is shown in the lower-left pictorial UT-OT diagram of Fig. 796, while on the lower-right is shown its associated UT-OT grid-diagram. This resulting braid is a kind of tubular flat braid that cannot take the shape of a round braid, in fact it appears as a beautiful flat braid.

If we had left at the joints the back-facing strings behind the front-facing strings we would have finished up with an UT-OT braid that can take the shape of a round braid. This UT-OT braid is shown by its UT-OT grid-diagram at the left in Fig. 797, while the conventional grid-diagram of this braid as a round braid is shown on the right in Fig. 797. Thus by braiding this round braid as an UT-OT braid while changing the string-run coding locally at the joint positions so as to comply with that shown in the lower-right diagram of Fig. 796, we obtain the tubular flat braid depicted there.

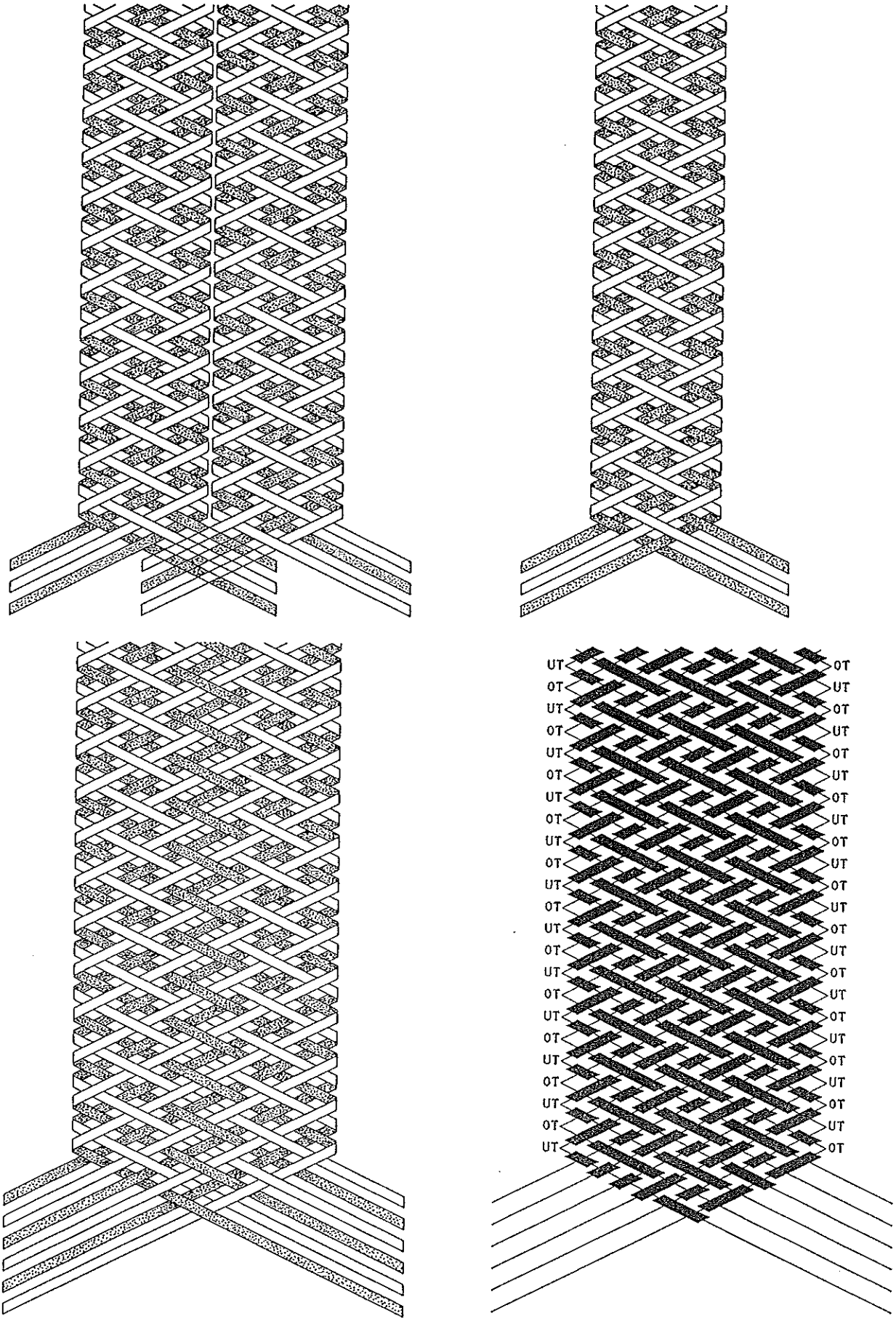

Fig. 796 —The development of a simple 12-lead tubular flat braid.

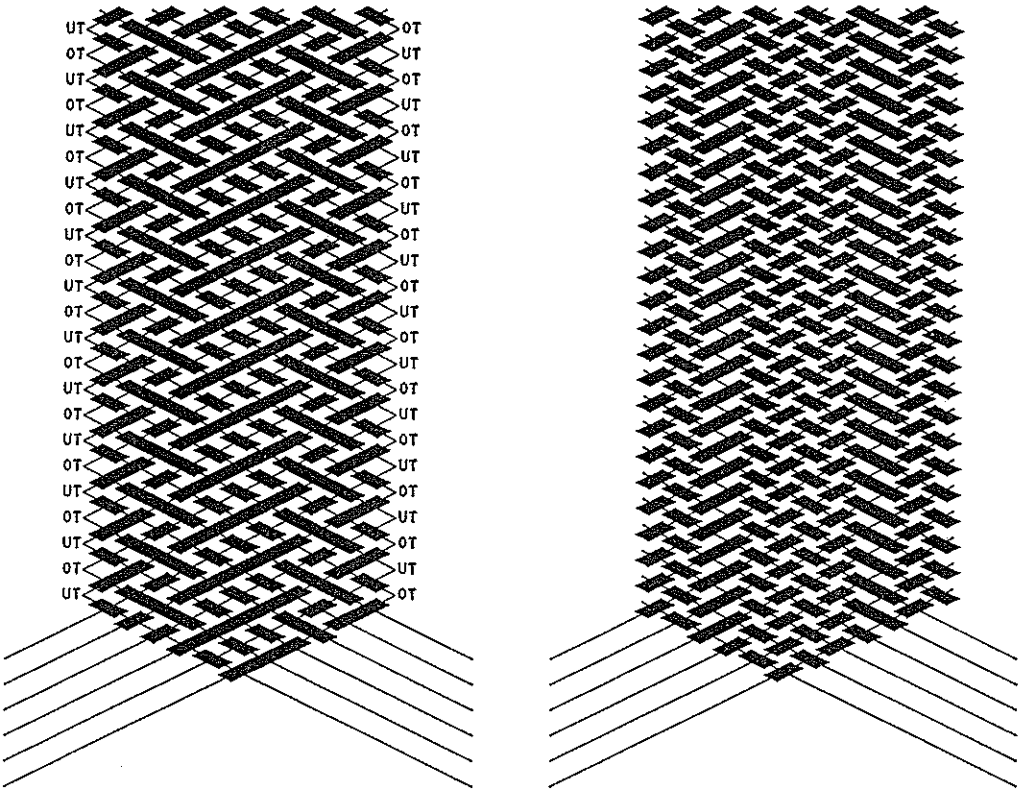

Fig. 797 — The associated 12-lead primitive flat tubular UT-OT braid and its conventional grid-diagram as a round braid.

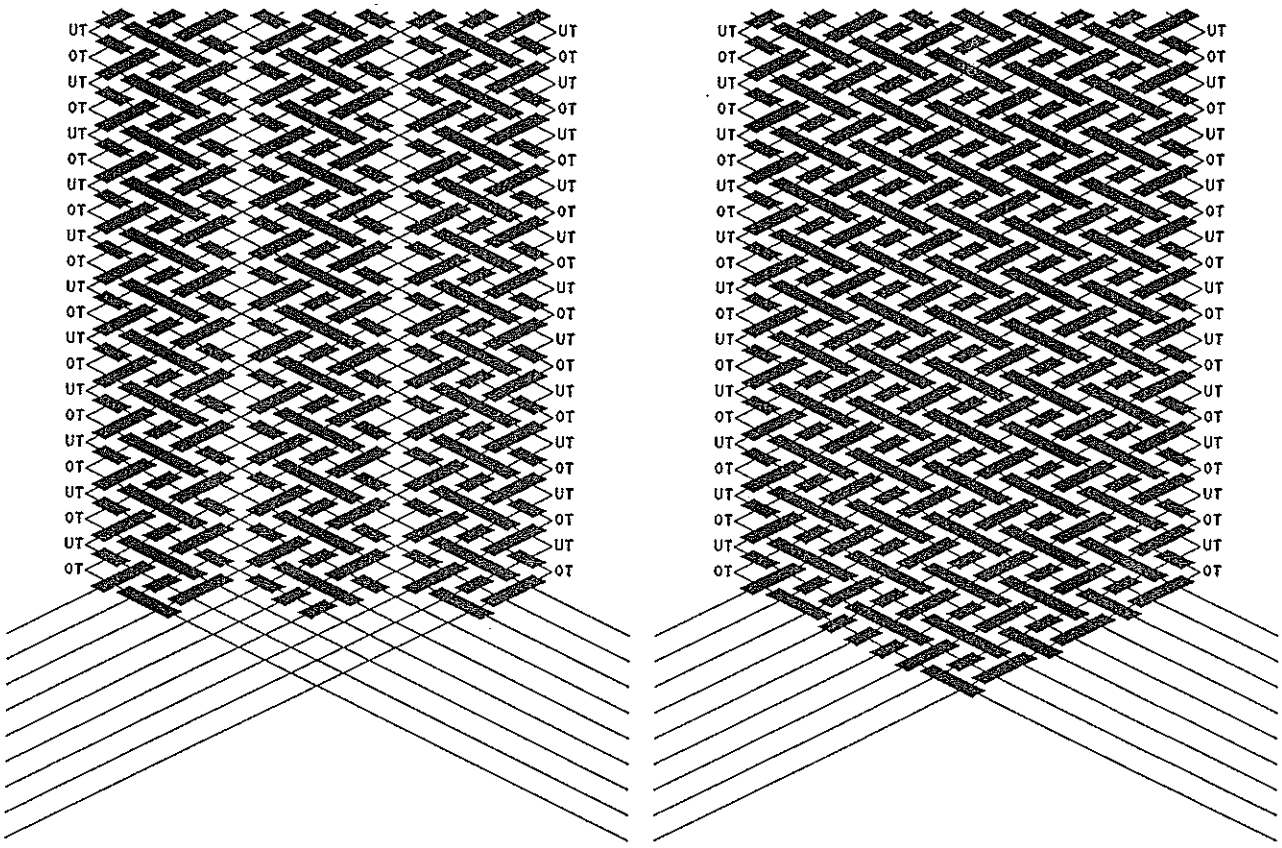

Fig. 798 — The development of a simple 18-lead tubular flat braid.

In Fig. 798 we have placed three of the UT-OT braids in Fig. 795 side by side and joined them together as in Fig. 796. The resulting braid is a beautiful tubular flat braid.

If we had again left at the joints the back-facing strings behind the front-facing strings we would have finished up with an UT-OT braid that can take the shape of a round braid. This UT-OT braid is shown by its UT-OT grid-diagram at the left in Fig. 799, while the conventional grid-diagram of this braid as a round braid is shown on the right in Fig. 799. Thus by braiding this round braid as an UT-OT braid while changing the string-run coding locally at the joint positions so as to comply with that shown in the right diagram of Fig. 798, we obtain the tubular flat braid depicted there.

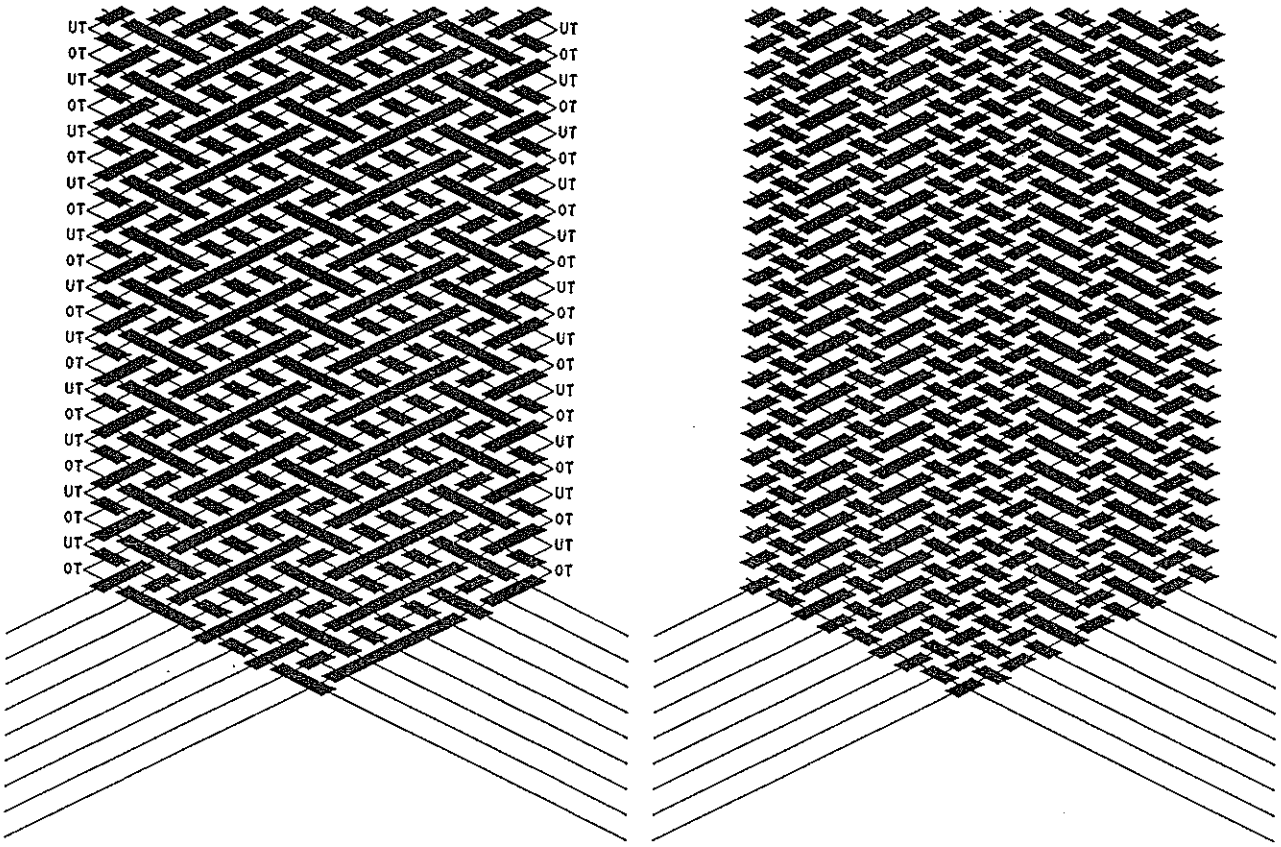

Fig. 799 — The associated 18-lead primitive flat tubular UT-OT braid and its conventional grid-diagram as a round braid.

The upper-right conventional round braid grid-diagram in Fig. 800 shows the under-over coded 4-lead round braid while its two UT-OT forms are shown to its left. When we place again two UT-OT grid-diagrams side by side, then for a balanced joint arrangement we need to use both these two UT-OT grid-diagram forms as shown on the lower-left in Fig. 800. After observing the same joining procedure as before, we obtain the lower-right UT-OT grid-diagram in Fig. 800. The resulting braid is again a beautiful tubular flat braid.

If we had left at the joints the back-facing strings behind the front-facing strings we would have finished up with an UT-OT braid that can take the shape of a round braid. This UT-OT braid is shown by its UT-OT grid-diagram at the left in Fig. 801, while the conventional grid-diagram of this braid as a round braid is shown on the right in Fig. 801. Thus by braiding this round braid as an UT-OT braid while changing the string-run coding locally at the joint positions so as to comply with that shown in the

lower-right diagram of Fig. 800, we obtain the tubular flat braid depicted there.

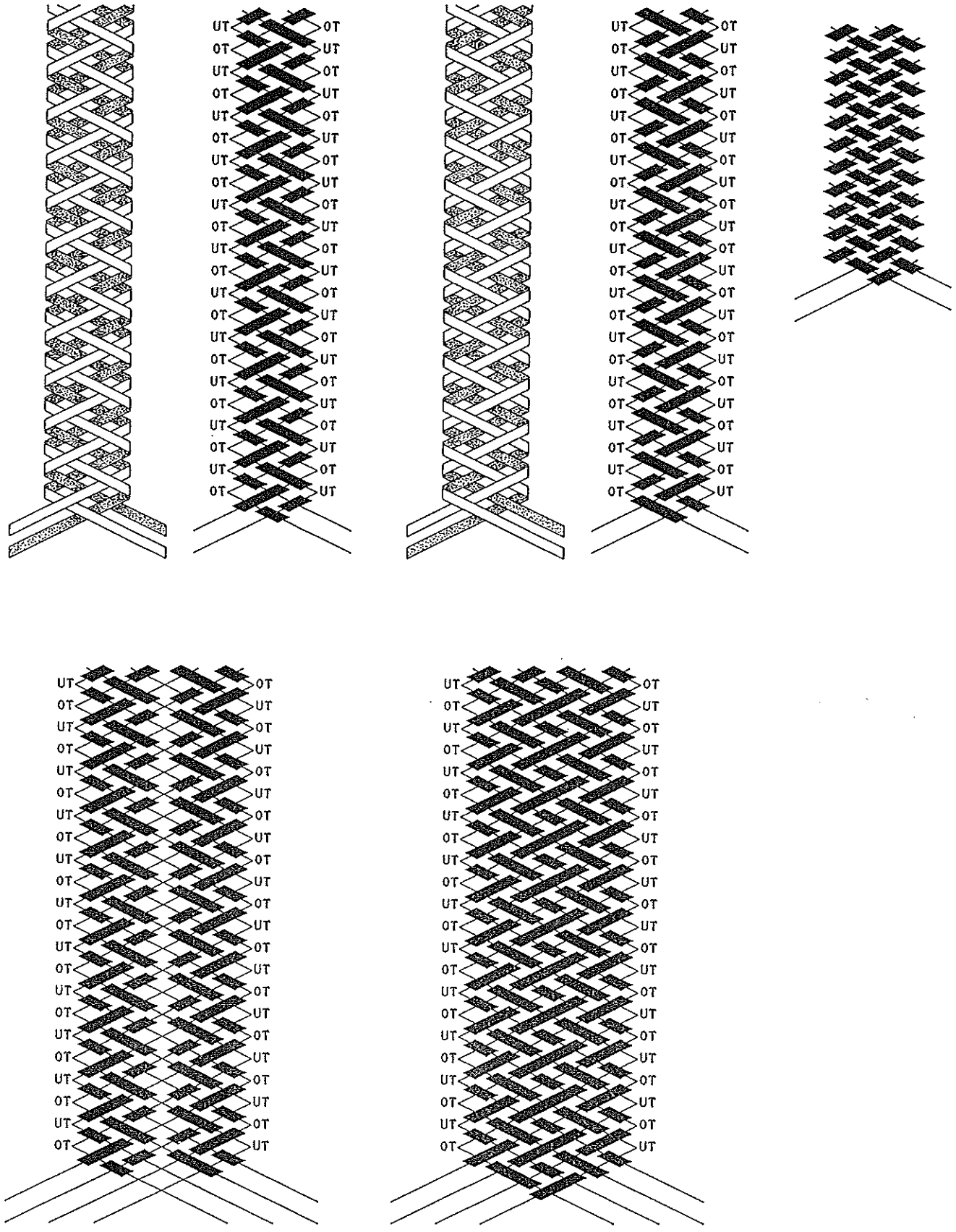

Fig. 800 — The development of a simple 8-lead tubular flat braid.

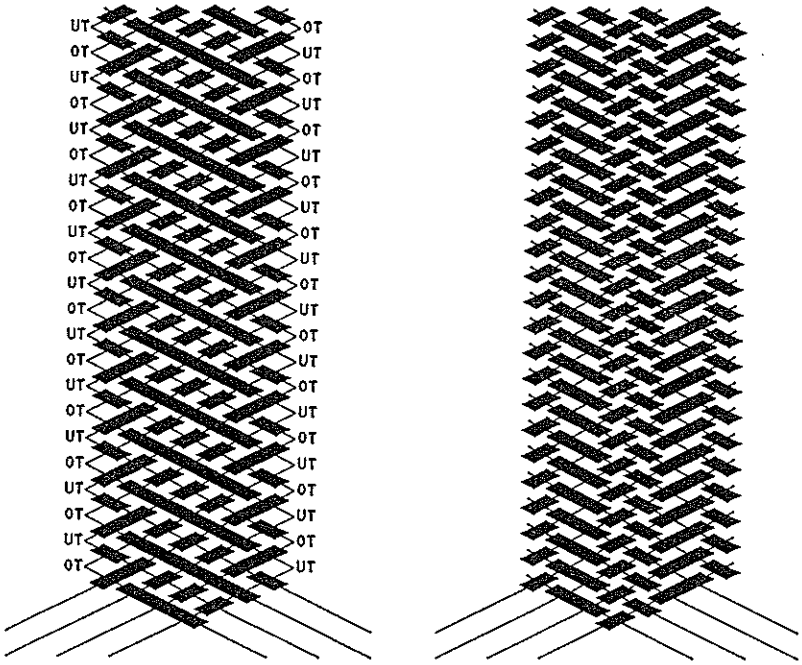

Fig. 801 — The associated 8-lead primitive flat tubular UT-OT braid and its conventional grid-diagram as a round braid.

In Fig. 802 we have added a further UT-OT braid to the right-hand side of the lower-left arrangement in Fig. 800. For a balanced joint arrangement this further UT-OT braid must be of the same form as the leftmost one. After observing the same joining procedure as before, we obtain the UT-OT grid-diagram on the right in Fig. 802. The resulting braid is again a beautiful tubular flat braid.

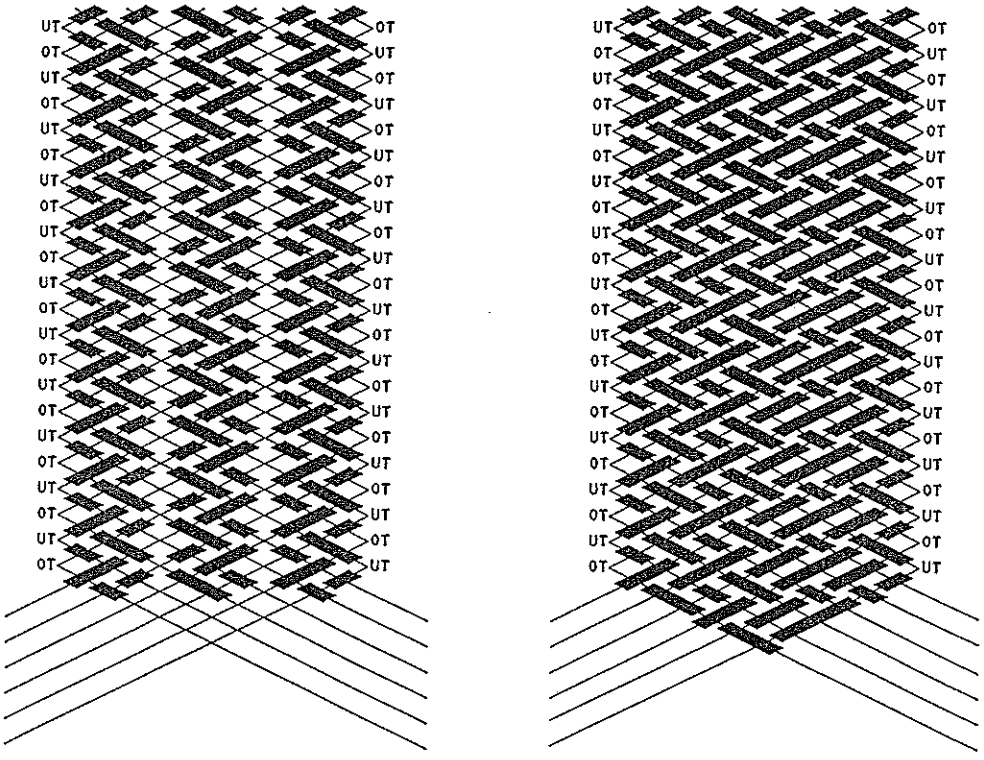

Fig. 802 — The development of a simple 12-lead tubular flat braid.

If we had left at the joints the back-facing strings behind the front-facing strings we would have finished up with an UT-OT braid that can take the shape of a round braid. This UT-OT braid is shown by its UT-OT grid-diagram at the left in Fig. 803, while the conventional grid-diagram of this braid as a round braid is shown on the right in Fig. 803. Thus by braiding this round braid as an UT-OT braid while changing the string-run coding locally at the joint positions so as to comply with that shown in the lower-right diagram of Fig. 802, we obtain the tubular flat braid depicted there.

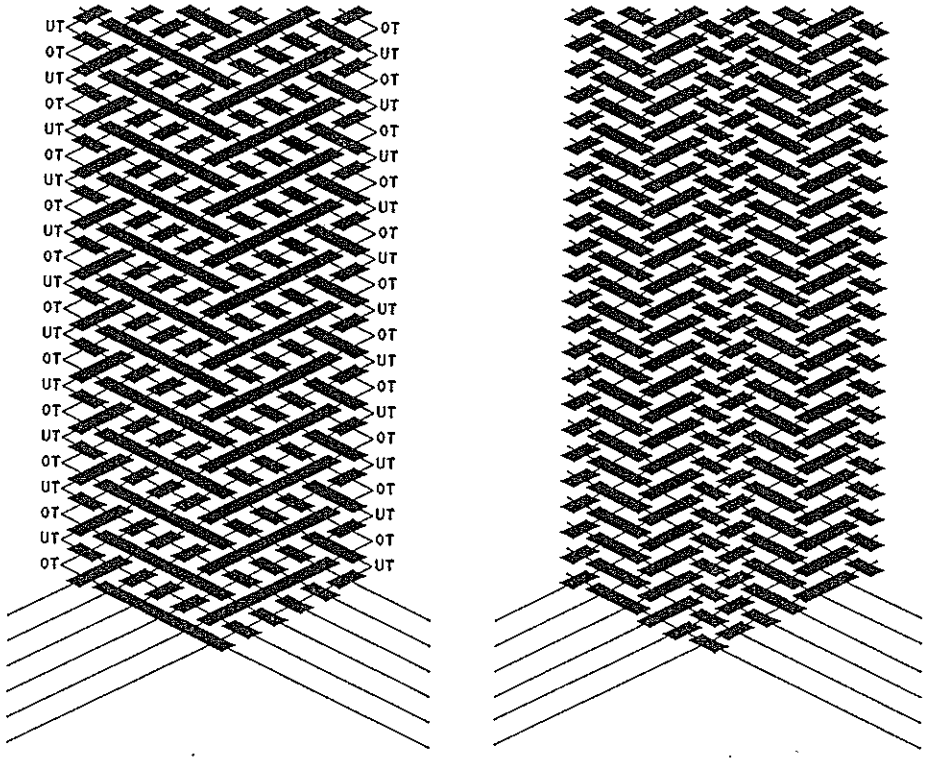

Fig. 803 — The associated 12-lead primitive flat tubular UT-OT braid and its conventional grid-diagram as a round braid.

As mentioned earlier, every under-over coded round braid has two different UT-OT grid-diagrams, hence two under-over coded primitive flat tubular UT-OT braid-forms. In the examples above of joining two or three under-over coded primitive flat tubular UT-OT braids, each with the same number of leads, we took the option for a front-facing string of a left helix in the leftmost of them to start at the left with an under.

Note that an under-over coded UT-OT braid does not show an under-over coding in its UT-OT grid-diagram. The codings shown are the codings of the actual string-crossings as well as of the virtual string-crossings.

⋆⋆ *Show that under an overall balanced and balanced joint construction procedure, a start at the left with an* **over** *for a front-facing string of a left helix in the leftmost under-over coded primitive flat tubular UT-OT braid creates the same UT-OT tubular flat braids as a start at the left with an* **under** *for a front-facing string of a left helix in the leftmost under-over coded primitive flat tubular UT-OT braid.*

Although we have kept here to the most simple tubular flat braids, tubular flat braids with a large variety of coding-patterns can be designed in a similar way. Furthermore, the tubular flat braids lead to 'new' forms of cylindrical braids — the **tubular flat torus braids.**